Natural Hazards
https://doi.org/10.1007/s11069-025-07551-2

REVIEW ARTICLE

Landslide-triggered tsunamis – a review

Katrin Dohmen[1] · **Philipp Blum**[2] · **Anika Braun**[1] · **Tomas Manuel Fernandez-Steeger**[1]

Received: 14 March 2025 / Accepted: 22 July 2025

Abstract
Risk mitigation for landslide-triggered tsunamis (LTT) is impeded by high uncertainty regarding the location of triggering landslides and the expected wave heights. Hence, this review aims to comprehensively analyze the spatial distribution, landslide characteristics, generated wave heights, and impact on humans of 317 LTT published as a catalog in a data repository (Dohmen et al. 2025). A classification system for LTT is established based on the preparatory and triggering factors of the landslides: (1) earthquakes, (2) volcanic activity, (3) paraglacial conditions, (4) precipitation, (5) anthropogenic activities, and (6) unknown causes. LTT triggered by earthquakes and volcanic activity are the most frequent classes and account for the highest fatalities and greatest economic damage. The highest waves are generated in enclosed marine environments and inland waters, often caused by anthropogenic activities such as reservoir operations. To mitigate risks from LTT, it is essential to know the exact location of the triggering landslide before failure, which is not the case for most events. As data availability is limited for landslide characteristics—especially in submarine environments—there is a need for high-resolution bathymetric data to map and investigate tsunamigenic submarine landslides and link them to expected tsunami heights and potential impacts on coastal populations. Offshore landslide susceptibility mapping is therefore recommended as a promising approach for identifying potential LTT failure locations.

Keywords Landslide tsunami · Tsunami · Coastal landslide · Submarine landslide · Mitigation

✉ Anika Braun
anika.braun@tu-berlin.de

[1] Institute of Applied Geosciences, Technische Universität Berlin, Ernst-Reuter-Platz 1, 10587 Berlin, Germany

[2] Karlsruhe Institute of Technology (KIT), Institute of Applied Geosciences (AGW), Kaiserstraße 12, 76131 Karlsruhe, Germany

Published online: 09 October 2025

1 Introduction

Besides earthquakes, landslides are the second most frequent source of tsunamis. Approximately 10% of all tsunamis observed globally have been triggered by landslides or by a combination of landslides, earthquakes, and volcanic activity (National Geophysical Data Center 2024). The term *landslide-triggered tsunamis (LTT)* refers to waves generated by all types of landslides and in various water bodies. It encompasses the designation *impulse wave*, which is often used in other studies to describe waves generated by subaerial landslides into inland waters (e.g., Fritz et al. 2004; Crosta et al. 2016; Chen et al. 2024). Landslides that have triggered tsunamis in the past—or have the potential to do so—are referred to as *tsunamigenic landslides* (Huene et al. 1989).

While LTT can generate waves higher than those produced by seismic tsunamis, their far-field propagation is usually limited (Okal and Synolakis 2003). Ferrer and González-de-Vallejo (2024) investigated so-called megatsunamis—waves of exceptional height—and concluded that landslides are the only trigger capable of producing tsunamis higher than 32 m. In 1958, a coseismic landslide into Lituya Bay, Alaska, triggered waves up to 524 m that ran up the opposite slope—the highest ever recorded (Fig. 1, no. 2; Fig. 2a). At the entrance to the bay, approximately 12 km from the landslide, the wave had already attenuated to a height of only 9 m (Miller 1960). LTT events have caused fatalities in various parts of the world, including both ocean coasts and inland waters, across all continents and

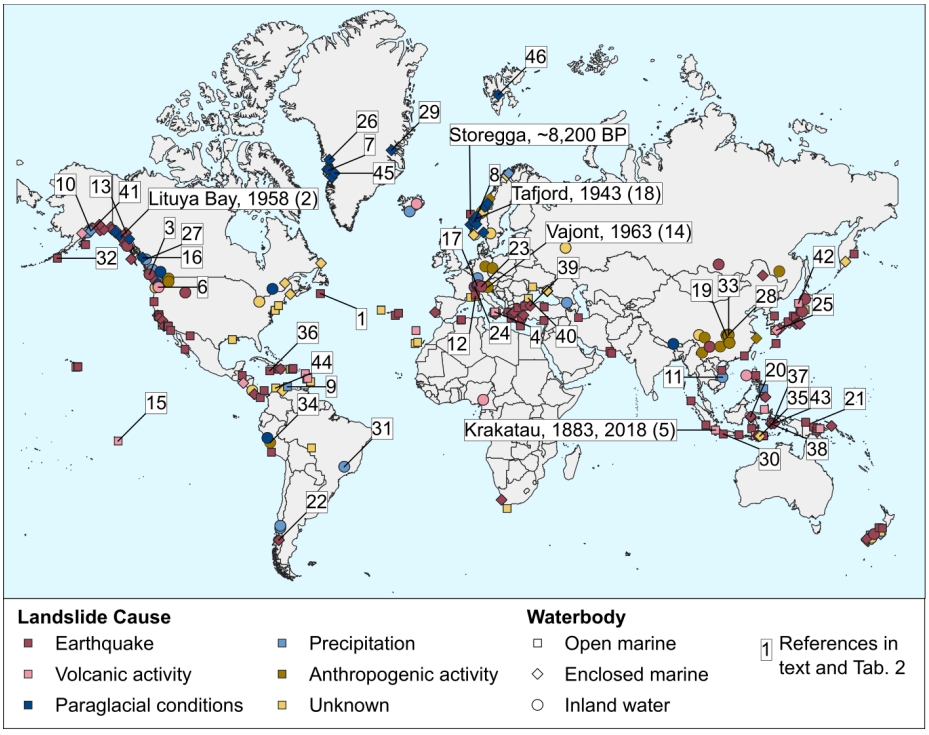

Fig. 1 Global spatial distribution of LTT. Symbol colors indicate the landslide cause, while symbol shapes represent the type of water body where the tsunami occurred. LTT events referenced in the text are labeled. Events numbered 1 to 17 are further described in Table 2

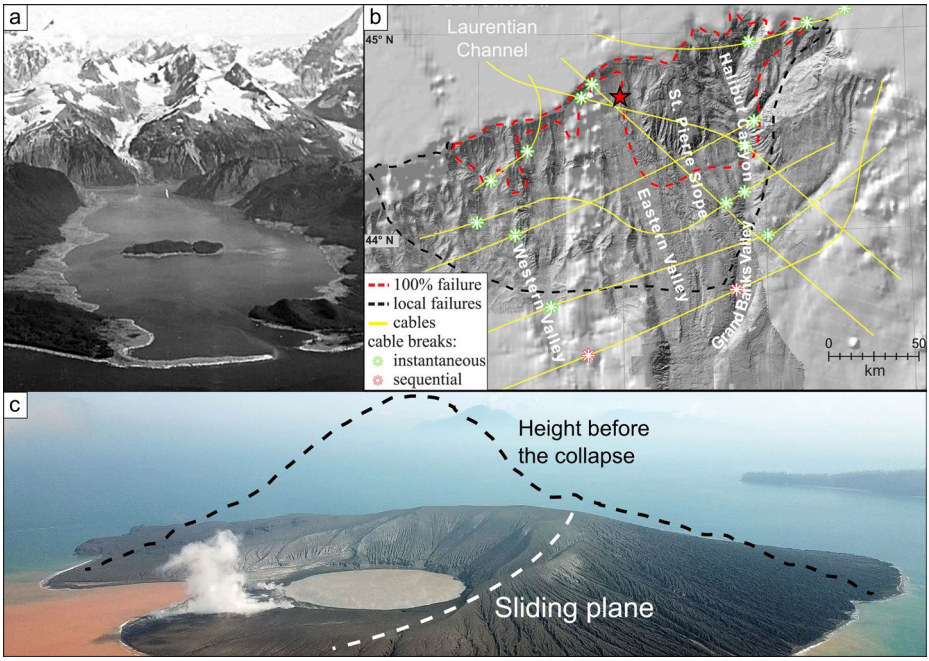

Fig. 2 Examples of historical LTT that are comprehensively documented in the literature: **a**) Trim lines in Lituya Bay, Alaska, following the 1958 event (courtesy of the U.S. Geological Survey; photo by Don J. Miller; see Fig. 1, no. 2). **b**) Bathymetric map showing the Grand Banks submarine landslide offshore Newfoundland, Canada, and the associated submarine cable breaks. The red star marks the location of the triggering earthquake (Schulten et al. 2019; Fig. 1, no. 1). **c**) Drone image of Anak Krakatau after the 2018 flank collapse (source: GFZ German Research Centre for Geosciences 2019). The black dashed line indicates the former extent of the volcanic edifice, which was reduced in height from 320 m to 120 m a.s.l. (Walter et al. 2019; Fig. 1, no. 5)

under diverse geological and climatic conditions. For example, in April 1934, 1.5×10^6 m³ of rock fell into Tafjord, Norway, generating 62 m high waves that killed 42 people (Harbitz et al. 1993; Waltham 2002; Hermanns et al. 2006; Panthi and Nilsen 2006; Fig. 1, no. 18). Another example is the Dayantang landslide in China: water level variations within the Shuibuya Reservoir triggered a 3×10^6 m³ landslide that induced 50 m high waves, drowning 8 people in 2007 (Yang et al. 2014; Wang et al. 2021c; Fig. 1, no. 19).

Developing early warning systems or implementing mitigation measures for LTT is challenging for two main reasons. First, most tsunamigenic landslides occur directly at the coastline or very close to it (Du et al. 2025). As a result, the time between landslide initiation and wave arrival at the nearest coastal community—where wave heights and associated impacts are greatest—is typically too short for effective warning and evacuation. For example, the waves triggered by coseismic landslides during the 2018 Sulawesi earthquake in Indonesia reached the shores of Palu Bay approximately 100 s after the earthquake (Carvajal et al. 2019; Fig. 1, no. 20). The second challenge lies in the high uncertainty surrounding tsunami characteristics (Løvholt et al. 2020). A variety of parameters influence the properties of the generated tsunami waves (Løvholt et al. 2015), making them difficult to compare. Meanwhile, submarine landslides are rarely studied in detail due to their limited

accessibility (Roger et al. 2024). Consequently, the timing, location, and characteristics of the triggering landslides often remain unknown.

Research interest in LTT has steadily increased since 1998, when a submarine landslide generated a tsunami that killed 2,100 people in Papua New Guinea (Synolakis et al. 2002; Fig. 1, no. 21). A further rise in scientific attention occurred after two LTT events in Indonesia caused numerous casualties in 2018. On September 28 of this year, during the Sulawesi earthquake (see above), coseismic landslides triggered tsunami waves up to 10 m high, resulting in nearly 2,000 fatalities (e.g., Muhari et al. 2018). On December 22, 437 people were killed when the flank of Anak Krakatau volcano collapsed into the ocean between Java and Sumatra (Grilli et al. 2019; Fig. 1, no. 5; Fig. 2c). More recently, glacial retreat accelerated by climate change has drawn increased attention to LTT along fjord coastlines; for example, in Greenland and Alaska, where glacial debuttressing alters stress fields and promotes landslides into fjords (Walden et al. 2025). One remarkable case occurred on September 16, 2023, when a rockslide into Dickson Fjord, Greenland, generated a 200 m high wave. The resulting seismic signal was detectable globally for over a week, likely due to a standing wave sloshing back and forth within the fjord (Carrillo-Ponce et al. 2024; Svennevig et al. 2024; Fig. 1, no. 29).

Most scientific studies on LTT focus on individual case studies from a phenomenological perspective (e.g., Rabinovich et al. 1999; Ioualalen et al. 2010; Corsa et al. 2022; Pedrosa-González et al. 2022; Chen et al. 2023). However, several reviews have been published in recent years. Couston et al. (2015) and Kremer et al. (2021) reviewed LTT in lakes and inland waters; Roberts et al. (2014) compiled a preliminary catalog of LTT from subaerial landslide sources; Roger et al. (2024) and Du et al. (2025) recently focused on submarine landslide-induced LTT; lastly, volcanic tsunamis have been reviewed by Paris et al. (2014) and Schindelé et al. (2024). While these reviews address specific types of LTT, coastal communities can be exposed to multiple types of tsunamigenic landslides. For example, LTT along the Indonesian coast can be triggered by both earthquakes and volcanic activity. To develop effective mitigation strategies, a comprehensive understanding of LTT hazards is needed, particularly concerning expected magnitudes, probabilities, and origins of events that may affect a given community (Alberico et al. 2018; Spahn and Lauterjung 2023). Therefore, it is essential to investigate all types of LTT, regardless of the triggering mechanism, water body, submarine or subaerial origin, or wave height.

To address the current knowledge gaps, we developed a global database of LTT (Dohmen et al. 2025). A total of 317 cases were reviewed concerning landslide properties and causes, generated wave heights, and the resulting economic damage and fatalities in affected coastal communities. In this study, we present a statistical analysis of this comprehensive database, linking landslide parameters with water body types and tsunami wave heights on a global scale. We identify the most frequent LTT triggers, the locations where the highest waves are generated, and the regions experiencing the most severe consequences in terms of fatalities and economic losses. These insights help evaluate mitigation options tailored to different LTT types. The database represents a significant step toward understanding the threats posed by LTT to coastal populations. Knowledge of past LTT events in a given region offers valuable insights into the likelihood and potential impact of future occurrences, supporting preparedness and mitigation planning in vulnerable coastal areas.

2 Types of LTT

2.1 LTT database compilation

2.1.1 Data sources

Historical LTT data were compiled from a wide range of sources, as summarized in Table 1. All documented LTT cases available up to October 30, 2024, were considered. The initial compilation resulted in 355 entries. Of these, 38 cases were excluded from the statistical analysis and classified as *not suitable*. These exclusions were due to incorrect entries in the original sources, a lack of supporting evidence for a landslide origin in the literature, or more recent studies disproving a landslide-triggered mechanism. An additional 20 entries refer to tsunamis generated by multiple landslides, such as the 2007 event in Aysen Fjord, Chile, which was triggered by several coseismic slope failures (Naranjo et al. 2009; Sepúlveda and Serey 2009; Sepúlveda et al. 2010; Lastras et al. 2013; van Daele et al. 2013; Fig. 1, no. 22). Each of these entries includes landslide-specific data; however, since tsunami wave heights, fatality counts, and economic losses cannot be attributed to individual landslides, identical tsunami impact data are assigned to all related entries. Consequently, the final database comprises 317 distinct landslides responsible for triggering 297 tsunami events.

Landslides that trigger tsunamis are classified according to their primary cause (Fig. 3): (a) earthquakes, (b) volcanic activity, (c) paraglacial conditions, (d) precipitation, (e) anthropogenic activity, and (f) unknown. Identifying the exact trigger can be difficult; even with intensive field investigations, it is often not possible to determine a definitive cause. When LTT events occur during or immediately following earthquakes, volcanic eruptions, or intense precipitation, the landslides are assigned to the corresponding category. If none of

Table 1 Sources used for compiling the LTT database. The references listed are representative examples; the complete list is provided in Dohmen et al. (2025)

Type of source	Examples and references
Tsunami databases	*Global Historical Tsunami Database* (National Oceanic and Atmospheric Administration, USA, National Geophysical Data Center 2024). *Global Historical Tsunami Database* (Tsunami Laboratory, Novosibirsk, Russia, TL/ICMMG 2024). *New Zealand Tsunami Database* (Downes et al. 2017).
Tsunami catalogs	Iida et al. 1967; Soloviev and Go 1974, 1975; Papadopoulos and Chalkis 1984; Lander et al. 1993; Lander 1997; Soloviev et al. 2000; Lander et al. 2002, 2003; Papadopoulos et al. 2007; Hermanns et al. 2014; Maramai et al. 2014; Roberts et al. 2014; Harris and Major 2017; Dirección General del Instituto Geográfico Nacional 2023.
Peer-reviewed articles on single case studies	Mitchell 1954; Tinti et al. 2005; Zhou et al. 2016; Gauthier et al. 2018; Liu et al. 2020; Aránguiz et al. 2023.
Book chapters	Plafker and Eyzaguirre 1979; L'Heureux et al. 2014.
Technical reports	Coulter and Migliaccio 1966; Seed et al. 1988; Gardner et al. 2001.
News articles	Rudolphi 2023; Neumann 2023.
Blog posts	Petley 2009, 2020, 2022.

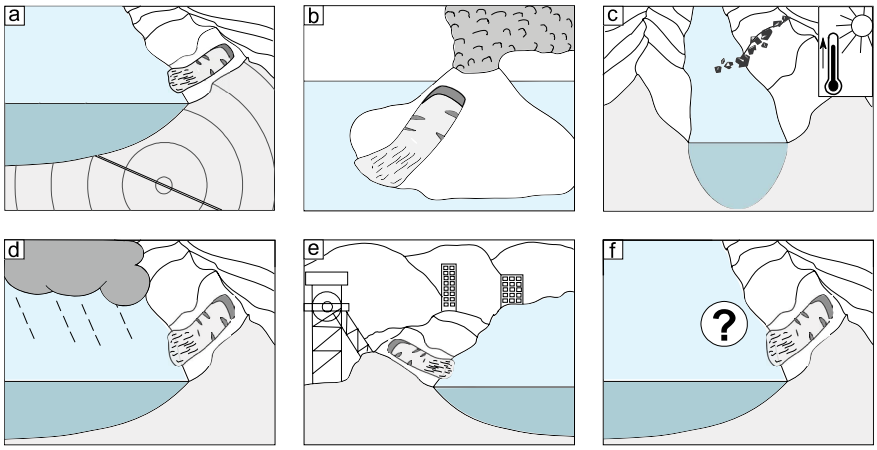

Fig. 3 Classification of causes of LTT: (**a**) earthquakes, (**b**) volcanic activity, (**c**) paraglacial conditions, (**d**) precipitation, (**e**) anthropogenic activity, and (**f**) unknown

these three triggers are evident, classification is based on preparatory factors that contribute to slope instability. Observations indicate that a significant number of tsunamigenic landslides are associated with anthropogenic activity or paraglacial conditions—that means the transitional processes following glacial retreat. Events that cannot be clearly attributed to any of the above causes are categorized as *unknown*. In addition to the causing mechanism, LTT events are also categorized by the type of water body in which they occur: (1) open marine environments, (2) enclosed marine environments, and (3) inland waters.

The literature on each documented case study was reviewed to compile information on landslide properties, generated tsunami heights, and tsunami consequences. Table 2 presents one exemplary case from each combination of landslide causes and water bodies. Landslide locations are classified as (1) subaerial, (2) submarine, and (3) partially submerged, for landslides whose origin is partly above and partly below the water surface. Following the classification system proposed by Hungr et al. (2014), landslide types were categorized as (1) fall, (2) topple, (3) slide, (4) spread, (5) flow, or (6) slope deformation. Two additional classes were added due to their relative frequency in LTT-related literature: (7) volcano flank collapse and (8) coastal subsidence. Volcano flank collapses are difficult to classify because they can involve complex processes with multiple sliding mechanisms (Paris et al. 2014). The term coastal subsidence is typically used in LTT literature related to seismic activity, where parts of the coastline slide into the water; however, the landslide motion is often not investigated in detail (e.g., Papadopoulos et al. 2007; Arikawa et al. 2018; Liu et al. 2020). Lithological information is generally poorly documented for most landslides. Therefore, landslide material is broadly classified as (1) soft rock, (2) hard rock, or (3) ice. The landslide volume is classified according to the scheme by McColl and Cook (2024): (1) very small (<1 m³), (2) small (1–10^3 m³), (3) medium (10^3-10^6 m³), (4) large (10^6-10^9 m³), (5) giant (10^9-10^{12} m³), and (6) monster ($>10^{12}$ m³).

Tsunami height is typically described using two different parameters. The maximum tsunami height refers to the highest local watermark relative to the undisturbed water level at the time of the tsunami. The maximum run-up height is the vertical difference between the undisturbed water level at the time of the tsunami and the highest point of inland tsunami

Table 2 Key parameters for selected case studies

Landslide cause[1]	Water body	Case study (year)[2]	Country	Landslide location	Landslide type	Landslide material	Landslide volume [10^6 m³]	Run-up [m]	Fatalities	Damage[3] [10^6 US$]	Reference
EQ	OM	Grand Banks (1929)[1]	Canada	submarine	slide	soft	175,000	13	28	1–5	Fine et al. (2005)
EQ	EM	Lituya Bay (1958)[2]	USA	subaerial	fall	hard	30.6	524	2	<1	Miller (1960)
EQ	IW	Mt Colonel Foster (1946)[3]	Canada	subaerial	avalanche	hard	0.7	51	0	<1	Evans (1989)
V	OM	Stromboli (2002-1)[4]	Italy	partially submerged	volcano flank collapse	hard	12	10.9	0	1–5	Tinti et al. (2005)
V	EM	Krakatau (2018)[5]	Indonesia	partially submerged	volcano flank collapse	hard	220	13.5	437	>25	Walter et al. (2019)
V	IW	Spirit Lake (1980)[6]	USA	subaerial	fall	hard		260			Sosio et al. (2012)
PA	EM	Paatuut (2000)[7]	Greenland	subaerial	avalanche	hard	30	50	0	<1	Dahl-Jensen et al. (2004)
PA	IW	Lake Loen (1905)[8]	Norway	subaerial	fall	hard	0.35	40.5	61	1–5	Waltham (2002)
PR	OM	Venezuela (1979)[9]	Venezuela	submarine					0	<1	Schubert (1994)
PR	EM	Pedersen Lagoon (2024)[10]	USA	subaerial	slide	hard	2	17	0	<1	USGS (2024)
PR	IW	Truong River (2017)[11]	Vietnam	subaerial	slide	hard	0.03	8.5	1	<1	Duc et al. (2020)
A	OM	Nice (1979)[12]	France	submarine	slide	soft	10	10	10	<1	Seed et al. (1988)
A	EM	Skagway (1994)[13]	USA	submarine	slide	soft	0.80	11	1	>25	Rabinovich et al. (1999)
A	IW	Vajont (1963)[14]	Italy	partially submerged	slide	hard	270	260	2043	5–25	Barla and Paronuzzi (2013)
U	OM	Fatu Hiva (1999)[15]	French Polynesia	subaerial	slide	soft	3	8	0	<1	Okal et al. (2002)
U	EM	Kitimat (1975)[16]	Canada	submarine	flow	soft	55	8.2	0	1–5	Prior et al. (1982)
U	IW	Lake Brienz (1996)[17]	Switzerland	submarine	slide		2.27	0.5	0		Girardclos et al. (2007)

[1] EQ: Earthquake, V: Volcanic activity, PA: Paraglacial conditions, PR: Precipitation, A: Anthropogenic activity, U: Unknown, OM: Open marine, EM: Enclosed marine, IW: Inland water. [2] Superscript numbers refer to the labels in Fig. 1. [3] Data for damages were taken from the National Geophysical Data Center (2024)

propagation (Intergovernmental Oceanographic Commission 2019). In addition, the database includes a parameter called maximum water height, which represents the greater of the two: the maximum tsunami height and the maximum run-up height.

To evaluate tsunami consequences, the database includes two parameters. The number of fatalities was extracted from the literature and refers to the individuals confirmed to have been killed by the tsunami, as well as those reported missing and presumed to have been swept away. The tsunami damage value was adopted from the *Global Historical Tsunami Database* (National Geophysical Data Center 2024), which provides an estimated monetary value (in US dollars) for the damage caused by each tsunami. This value is categorized into 5 classes: (1) none (0 US$), (2) limited ($<1\times10^6$ US$), (3) moderate ($1–5\times10^6$ US$), (4) severe ($5–25\times10^6$ US$), and (5) extreme ($>25\times10^6$ US$). These classes are intended to reflect approximately current dollar values (National Geophysical Data Center 2024). Wherever possible, the database distinguishes fatalities and damage caused solely by the tsunami, excluding those attributable to the triggering event or the landslide itself.

2.1.2 Data availability

Figure 4 presents the data availability for the parameters compiled in the LTT database. The graphs display the data grouped by the causes of LTT, as described in detail in Sect. 2.3. Landslide parameters—including volume, material, type, and location—were recorded for 317 landslides (Fig. 4a), while tsunami parameters—damage, fatalities, and maximum water height—were recorded for 297 tsunamis (Fig. 4b). The availability of individual parameters within the database varies considerably.

Data availability is high for easily accessible parameters such as landslide location (89%), maximum water height (84%), and the number of fatalities caused by the tsunami (71%). For parameters requiring more detailed investigation, data availability is lower. Landslide type is available for 57% of cases, landslide material for 41%, and landslide volume for 35%. Determining the type or material of a landslide typically requires field investigations (e.g., Gusiakov and Makhinov 2021) and high-resolution digital elevation models (e.g., Gauthier et al. 2018). Landslide volume estimations rely on various methods, including field investigations (e.g., Zhang et al. 2019), aerial photo interpretation (e.g., Brideau et al. 2012), laser scans (e.g., Zhou et al. 2016), bathymetric surveys (e.g., Ioki et al. 2019), and tsunami back-propagation modeling (e.g., Heinrich et al. 2001). These methods are time-consuming, costly, and are often not applied, particularly in submarine environments or in cases where the tsunami caused no fatalities or damage, such as the 0.5 m high LTT that occurred in Seram, Indonesia, in 2021 (Fahmi et al. 2022; Heidarzadeh et al. 2022; Fig. 1, no. 43).

From Fig. 4, it is evident that information on landslide type, material, and volume is particularly lacking for earthquake-triggered LTT. Although this category accounts for 150 cases—the most frequent—data on landslide material, type, and volume are available for only 40, 59, and 32 events, respectively, resulting in an overall data availability of just 53% for earthquake-triggered LTT (Dohmen et al. 2025). For tsunamis caused by submarine landslides following earthquakes, data availability is even lower, with material, type, and volume known for only 6, 13, and 8 cases, respectively (Dohmen et al. 2025). In some earthquake-triggered LTT cases, there is no direct evidence of a landslide. Instead, the presence of a landslide is inferred from tsunami wave characteristics and the absence of other potential sources, without further investigation of the landslide itself. Similarly, data avail-

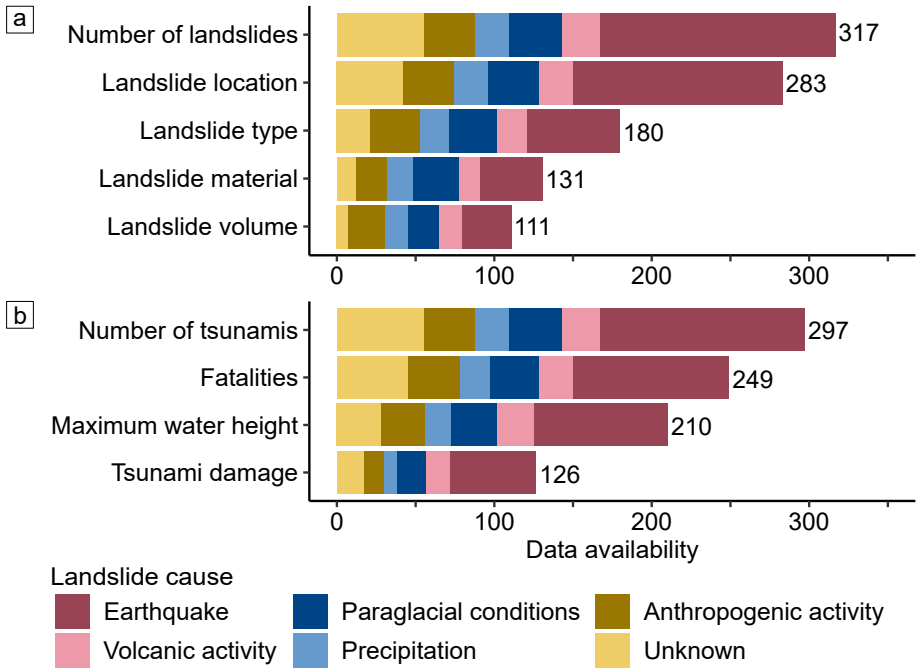

Fig. 4 Data availability of the parameters considered, categorized by the cause of LTT: **a**) landslide-related parameters, and **b**) tsunami-related parameters

ability for LTT with unknown causes is low, at just 45% (Dohmen et al. 2025). In most of these cases, the triggering landslide has not been investigated, while both its properties and origin remain unknown. In contrast, data availability is significantly higher for LTT triggered by paraglacial conditions (82%), precipitation (76%), volcanic activity (75%), and anthropogenic activity (79%) (Dohmen et al. 2025). Many anthropogenic LTT events are well studied due to their occurrence in densely populated areas or because they caused substantial damage or fatalities, thereby attracting public and scientific interest. Examples include the 1985 Xintan landslide, which entered the Yangtze River in China, resulting in 10 deaths and disrupting shipping traffic for 12 days (Huang et al. 2017; Fig. 1, no. 33), and the 1971 Chungar landslide and tsunami in Peru, which destroyed a mining camp with 600 workers and nearly all surface facilities (Plafker and Eyzaguirre 1979; Fig. 1, no. 34).

2.2 Spatial distribution of LTT

Figure 1 shows the global spatial distribution of LTT. LTT density is high along active tectonic margins, such as the Pacific Ocean and the Mediterranean Sea coasts, but relatively low along passive margins, including the coasts of Africa, Australia, and the western coasts of North and South America. High LTT density is also observed at high latitudes, such as in Norway, Canada, and New Zealand. LTT in inland waters occur primarily in reservoir lakes, particularly in China and the U.S. (Jones et al. 1961; Yang et al. 2017; Tang et al. 2019).

Despite relatively high landslide densities in mountainous regions, only a few LTT were observed in such environments. Several LTT have been documented in lakes of the Euro-

pean Alps; for example, Vajont (Barla and Paronuzzi 2013; Fig. 1, no. 14), Lake Sils (Nigg et al. 2021; Fig. 1, no. 23), and Lake Geneva (Kremer et al. 2012; Fig. 1, no. 24). However, very few LTT are recorded in other major mountain belts, such as the Himalayas or the Andes. This discrepancy may be partly due to the low population density in these regions, resulting in fewer reported LTT events. Another possible explanation involves terminology: many glacial lake outburst floods (GLOFs), often triggered by mass movements, are reported in these regions (Shrestha et al. 2023), but only a small number of these events appear in the literature as LTT.

Although the coast is characterized by elevated seismic activity from the active continental margin and high latitudes, which would suggest a raised LTT density, only very few LTT are documented on the west coast of South America (e.g., Aysen Fjord, Chile,2007, Sepúlveda et al. 2010). Völker et al. (2011) examined the bathymetry off Central Chile concerning seismicity and submarine landslide occurrence, concluding that regular earthquakes promote the formation of many small landslides. Due to their reduced size, these regular landslide processes do not pose a significant tsunami hazard. Furthermore, models on global sediment thickness show relatively low sediment accumulations for large parts of the South American Pacific coast (Straume et al. 2019), which could presumably result in a lower submarine landslide density. A very low LTT density is also observed in Africa, and not a single LTT has been reported in Australia, possibly due to a combination of relatively stable geologic conditions, low population density, and a lack of scientific interest.

2.3 LTT classification

2.3.1 Causes for landslide-triggered tsunamis

Most LTT are induced by earthquakes (Fig. 3a), with 44% (130 of 297) of all studied cases attributed to this category (Fig. 5). Seismic activity is generally a major trigger and preparatory factor for landslides (Keefer 1984, 2002; Fan et al. 2019), and thus also for LTT. Slopes are destabilized by ground shaking, increasing pore water pressure, and rock mass fracturing (Hack et al. 2007). Figure 2a shows an aerial image of Lituya Bay, Alaska, where earthquake-triggered LTT were documented in 1853, 1874, 1900, 1936, and 1958. The trim lines from the 1958 LTT, which generated 524 m high waves, are visible in the photograph (Miller 1960). Another example of an earthquake-caused LTT occurred offshore Newfoundland, Canada, in 1929. The bathymetric model in Fig. 2b shows the outline of the Grand Banks submarine landslide, triggered after an M_W 7.2 earthquake. The slide generated a tsunami with a water height of 13 m and killed 28 people (Fine et al. 2005; Fig. 1, no. 1).

About 8% (24 of 297) of the tsunamis in the database were induced by volcanic landslides Figs. 3b and 5). Volcanoes can trigger tsunami waves by several mechanisms; for example, earthquakes accompanying eruptions, pyroclastic flows, submarine explosions, or caldera collapses (e.g., Latter 1981; Paris et al. 2014; Di Traglia et al. 2022; Di Traglia et al. 2024). Volcanic tsunamis are often triggered by several mechanisms simultaneously, with it not always obvious which one has the strongest influence on wave generation (Paris et al. 2014). Only tsunami waves induced by volcanic landslides were considered in this study. There are many causes for landslide occurrences at volcanoes, both related and unrelated to volcanic activity. They include over-steeped, not buttressed flanks, buried faults, thermal alteration, pore pressure in the volcanic edifice, and the collapse of subaerial and submarine

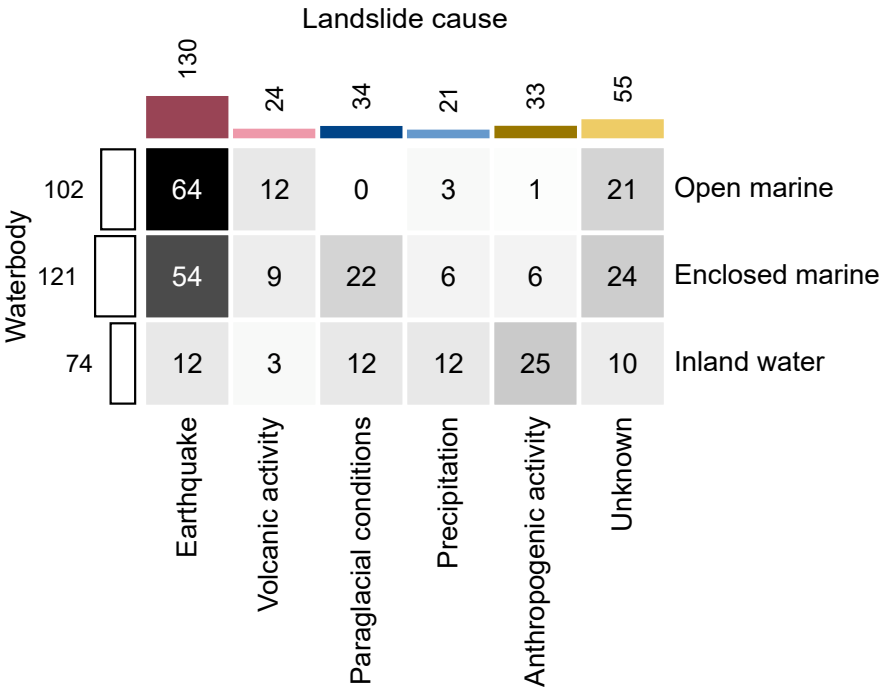

Fig. 5 Number of LTT case studies classified by landslide cause and type of water body

deposits (Keating and McGuire 2000). Volcano flank collapses can trigger extremely high waves, as was the case at Mt. Mayuyama volcano in Japan (Fig. 1, no. 25). In 1792, the volcano flank collapsed during a period of volcanic activity and slid into Ariake Bay in the western part of Kyushu. The generated waves reached a maximum run-up height of 20 m and killed about 10,000 people (Miyamoto 2010).

The causes of 11% (34 of 297) of all LTT in the database are attributed to paraglacial conditions (Fig. 5), which describe the transition from glacial to non-glacial environments (Fig. 3c). In general, these are not direct triggering factors, but rather a set of processes associated with glacial cycles, glaciation, and deglaciation that increase slope instability in both subaerial and submarine settings (McColl 2012). Particularly in the context of climate change, the expansion of paraglacial conditions due to glacier retreat may lead to increased slope destabilization in the future (Kim et al. 2022; Walden et al. 2025).

Subaerial slope stability can be reduced by several factors, including permafrost degradation (Davies et al. 2001; Matsuoka and Murton 2008), glacial thinning and retreat (Ballantyne 2002; Walden et al. 2025), very steep slopes resulting from glacial erosion (Caine 1982), exfoliation (Brunner and Scheidegger 1973), and seismicity caused by isostatic uplift (Fjeldskaar et al. 2000). Landslides occurring in quick clay are also commonly associated with paraglacial conditions, where isostatic uplift raises marine clays above sea level and the replacement of salt water with fresh water reduces shear strength through cation exchange (Rosenqvist 1953; L'Heureux et al. 2012; Hermanns et al. 2014; Liu et al. 2021). Typically, not just one but several of these processes act together to influence slope

stability and increase the prevalence of LTT under paraglacial conditions (McColl 2012). Another process that can trigger displacement waves in paraglacial conditions is glacier calving. Kostrzewa et al. (2024) show that this process occurs regularly and significantly shapes Arctic geomorphology. Although technically not a landslide process, glacier calving is included here because the National Geophysical Data Center (2024) database documents several tsunamis caused by the movement of ice masses. An example of an LTT induced by paraglacial conditions is the tsunami in Karrat Fjord, Greenland, in June 2017. Approximately 45×10^6 m³ of rock detached from an elevation of up to 1,200 m and entered the fjord at a very high velocity (Schiermeier 2017; Gauthier et al. 2018; Fig. 1, no. 26). The resulting waves reached several villages up to 160 km from the landslide. Some houses were washed away, while 4 people remain missing in Nuugaatsiaq, a village located about 32 km from the rockslide. The maximum wave run-up height at that distance is estimated to have been around 10 m (Paris et al. 2019).

In submarine environments under paraglacial conditions, glacial delta collapses are known triggers of tsunami waves (Prior et al. 1982; Harbitz et al. 2014). High sedimentation rates, particularly during glacier retreat, can produce thick layers of unconsolidated sediments prone to sliding and liquefaction (Coulter and Migliaccio 1966; Aarseth et al. 1989). Sedore et al. (2024) studied the controlling factors of submarine landslides in Nunavut, Canada, identifying additional causes in paraglacial settings, including seafloor over-steepening due to rapid sedimentation; subaerial debris flows or rockslides entering the water and destabilizing the seafloor; river flooding; and tidal loading. Furthermore, Normandeau et al. (2021) demonstrated that grounding icebergs can also trigger submarine landslides. An example of a glacial delta collapse occurred in 1975 in Kitimat Arm, British Columbia (no. 16 in Fig. 1; Table 2). The landslide, with an estimated volume of 2.3×10^6 m³, generated waves up to 8.2 m in height and caused severe damage along the local coastline. Several other landslides had been reported in Kitimat Arm before this event, between 1952 and 1975 (e.g., Prior et al. 1982; Kirby et al. 2016).

About 7% (21 of 297) of the documented LTT were caused by precipitation (Figs. 3d and 5), which is one of the main triggers of landslide events worldwide (Benz and Blum 2019). In subaerial environments, precipitation reduces slope stability by increasing soil saturation and pore water pressure (Wieczorek 1996). An example of a precipitation-triggered LTT occurred on the Truong River, Vietnam, in 2017. A slide with a volume of approximately 30,000 m³ generated a wave with a maximum run-up of 8.5 m, destroying six houses and killing one person (Duc et al. 2020; no. 11 in Fig. 1; Table 2).

Moreover, high precipitation rates can also trigger instabilities in submarine environments, where elevated river discharge resulting from heavy rainfall can both trigger and precondition submarine delta collapses (Clare et al. 2016; Sedore et al. 2024). According to Blais-Stevens et al. (2006), rapid sedimentation caused by intense precipitation likely triggered the 1998 Troitsa Lake tsunami in British Columbia, Canada (no. 27 in Fig. 1). In recent years, an increase in landslide activity has been observed in correlation with the rise in extreme rainfall events attributed to climate change (Kirschbaum et al. 2012; Gariano and Guzzetti 2016). Consequently, a future increase in precipitation-triggered LTT driven by climate change can reasonably be expected.

Approximately 11% (33 of 297) of all documented LTT were triggered by anthropogenic activity (Figs. 3e and 5). This category includes landslides affecting natural slopes due to human interventions—such as reservoir impoundment—as well as landslides occur-

ring at artificial embankments. The causes of embankment failures are diverse; they are often related to construction design but can also be triggered by natural processes such as heavy precipitation (Keqiang et al. 2008) or seismic activity (Heidarzadeh et al. 2023). Anthropogenic-triggered LTT have occurred on quarry slopes (Plafker and Eyzaguirre 1979; Xing et al. 2016), in open-pit mining lakes (Clostermann 2013; Katzenbach et al. 2013; Götz and Siebert 2020), and land reclamation sites (Assier-Rzadkieaicz et al. 2000; Zaniboni et al. 2014). LTT are regularly triggered at reservoir lakes worldwide, particularly along the shores of Franklin D. Roosevelt Lake in the United States (Jones et al. 1961) and the Three Gorges Reservoir in China (e.g., Tang et al. 2015). Since the impoundment of the Three Gorges Reservoir in 2003, several thousand landslides have been recorded in the surrounding area, with many triggered by high precipitation and fluctuating water levels. However, only a small fraction of these events have entered the reservoir and generated waves (Keqiang et al. 2010; Tang et al. 2019). Several slopes around the reservoir are currently being monitored due to ongoing movement, with their failure potentially having catastrophic consequences for the densely populated surrounding areas (Tang et al. 2015; Yang et al. 2017; Wang et al. 2021b). Reservoir water levels influence groundwater levels in adjacent slopes. Seasonal changes, as well as water level adjustments for economic or flood control purposes, can alter pore water pressure, thereby increasing the probability of slope destabilization (Tang et al. 2019).

Landslides occurring in reservoirs can not only generate tsunami waves that threaten nearby populations and infrastructure (Wang et al. 2021b), but the accumulation of landslide material within the reservoir can also significantly reduce its storage capacity. This reduction may compromise operational safety and result in substantial economic losses (Huang et al. 2019). The most well-known example of a reservoir-LTT is the 1963 Vajont landslide in northern Italy. Triggered by fluctuations in water level and intense rainfall, the landslide generated a wave with an estimated run-up height of approximately 260 m, resulting in 2,043 fatalities (Barla and Paronuzzi 2013; Fig. 1, no. 14).

For a significant proportion of documented LTT (19%, 55 of 297), the landslide cause is *unknown* (Figs. 3f and 5). Many of these events are relatively old, while either the landslide origin was never investigated in detail or the triggering mechanism can no longer be reliably identified. Cases in which the landslide origin was determined solely by excluding other potential causes were also classified as *unknown*. Most of these events occurred in submarine environments, where even the precise landslide location is uncertain and can only be approximated using bathymetric data and tsunami back-propagation modeling. One such example is the tsunami that occurred in Santa Marta, Colombia, in 2017 (National Geophysical Data Center 2024; Fig. 1, no. 44).

Tsunamis for which a landslide origin is considered a realistic scenario are also included, even if the triggering mechanism remains controversial. For instance, a sea disturbance was observed at multiple locations along the Bulgarian Black Sea coast in May 2007 (Fig. 1, no. 40). A seismic origin has been ruled out. According to Ranguelov et al. (2008), a submarine landslide may have caused the waves; however, Vilibić et al. (2010) argue that atmospheric conditions are the more likely trigger. In several cases, such as the 2012 tsunami in the Xianxi River, long-term physical weathering is believed to have led to the landslide, but no specific triggering event could be identified (National Geophysical Data Center 2024; Fig. 1, no. 28). These cases were also classified as *unknown*.

2.3.2 Waterbodies where LTT occurred

Of the 297 documented LTT, 34% (102 cases) occurred in open marine environments (Fig. 5), which are defined as coastal or marine areas with limited potential for wave reflection. In such settings, tsunami energy tends to dissipate rapidly due to the absence of major reflecting geometries. Open marine environments include, for example, landslides originating from straight shorelines, submarine landslides occurring on the continental slope far from the coastline, and events near isolated islands such as insular volcanoes. The documented causes of landslides in these settings are primarily earthquakes and volcanic activity; however, in some cases, the trigger remains unknown. Landslides caused by precipitation or anthropogenic activity are rare in open marine environments, and no LTT triggered by paraglacial conditions are observed in these areas.

Most cases of documented LTT (121 of 297, 41%) occurred in enclosed marine environments, which include narrow bays, fjords, or straits (Fig. 5). Their complex coastal geometry allows for increased refraction and reflection of tsunami waves. Tsunami energy in enclosed marine environments dissipates slowly because it is trapped within the water body (Couston et al. 2015). This was demonstrated impressively by the LTT in Dickson Fjord, Greenland, in September 2023, which generated a 7 m high seiche lasting 9 days within the enclosed fjord waters (Carrillo-Ponce et al. 2024; Svennevig et al. 2024; Fig. 1, no. 29). Earthquakes, paraglacial conditions, and *unknown* factors primarily caused LTT in enclosed marine environments. Landslides caused by volcanic activity, precipitation, and anthropogenic activity are uncommon.

25% (74 of 297) of all LTT occurred in inland waters such as lakes, rivers, and reservoirs (Fig. 5). Similar to enclosed marine environments, the potential for wave reflection and energy trapping is increased in inland waters. Furthermore, the short propagation distance within inland waters results in limited wave dissipation (Fuchs and Hager 2015). In contrast to marine environments, anthropogenic activity is the most significant cause of LTT in inland waters. Earthquakes, paraglacial conditions, precipitation, and unknown causes have also been identified as LTT causes. With only 3 reported cases, LTT triggered by volcanic activity are relatively uncommon in inland waters (Fig. 5). One example is the debris avalanche during the 1980 eruption of Mt. St. Helens into Spirit Lake, Washington State, which caused a wave with a run-up height of 260 m (Sosio et al. 2012; no. 6 in Fig. 1; Table 2).

2.4 LTT characteristics

2.4.1 Landslide statistics

Figure 6 shows the location, material, type, and volume of landslides that have triggered tsunamis in the past. Most documented LTT result from subaerial landslides (47%), followed by submarine (37%) and partially submerged (16%) landslides (Fig. 6a). Given the vast number of documented submarine landslides worldwide (e.g., Casalbore et al. 2011; Urgeles and Camerlenghi 2013; Brink and Geist 2021; Gamboa et al. 2021) and the fact that each landslide generates waves, it is reasonable to assume that many submarine LTT remain unrecognized. This could be due to landslides occurring far from the coast or the generated waves being too small to be noticed by coastal populations. Hence, a reporting bias in landslide location distribution is highly likely. The causes of subaerial landslides are

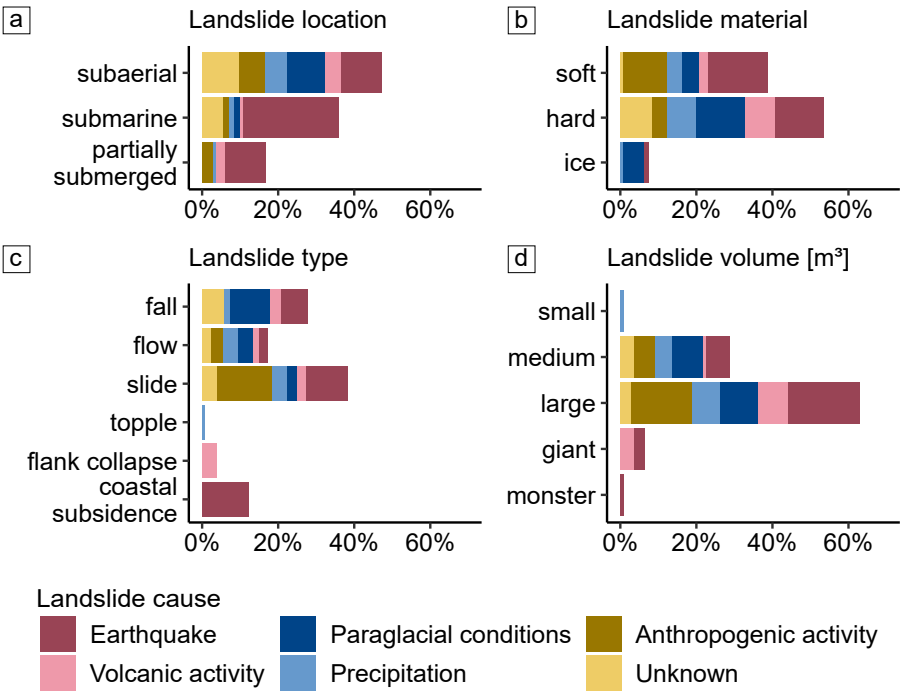

Fig. 6 Distributions of (**a**) location, (**b**) sliding material, (**c**) landslide type, and (**d**) volume of the studied LTT. Landslide volume classes refer to the scheme proposed by McColl and Cook (2024): small = 1–103 m^3, medium = $10^3 - 10^6$ m^3, large = $10^6 - 10^9$ m^3, giant = $10^9 - 10^{12}$ m^3, and monster > 10^{12} m^3

distributed evenly across the six classes, while submarine and partially submerged landslides were predominantly triggered by earthquakes. One reason for the high proportion of submarine earthquake-triggered LTT is the large number of case studies documenting unexpectedly high waves following earthquakes. Coseismic landslides are the assumed or proven triggers for these high waves. For example, during the 2006 South Java tsunami, run-up heights of 5–7 m were measured along the coasts, but extreme run-up heights locally exceeding 20 m were attributed to coseismic landslides (Fritz et al. 2007; Fig. 1, no. 30). Partially submerged landslides are mostly coastal subsidence events caused by earthquakes.

Most documented landslides consist of hard rock (53%), with a relatively large number of these triggered by paraglacial conditions (Fig. 6b). This can be explained by the high number of documented rockfall events at fjord coasts, which are one of the dominant coast types in paraglacially characterized regions (Forbes and Syvitski 2010). Soft rock landslides triggered 40% of the LTT in the database. Since all documented embankment failures occurred in soft rock, a large proportion of these soft rock landslides are caused by anthropogenic activity. Only a small proportion of tsunamis in the database are triggered by ice (7%); their only triggers are paraglacial conditions, earthquakes, and precipitation. Calving processes have been included in tsunami databases only in the last few years, resulting in a small number of landslides consisting of ice; for example, events in western Greenland in 2014 or in Svalbard in 2011 (Marchenko et al. 2012; Lüthi and Vieli 2016; Fig. 1, no. 45 and 46).

The most frequently documented landslide type is slide, accounting for 39%, followed by fall (27%), flow (18%), and coastal subsidence (12%) (Fig. 6c). The database contains few LTT associated with flank collapses (4%) or topples (1%). Slide-type landslides are frequently triggered by anthropogenic activities. Embankment failures are one type, where embankments—typically made of homogeneous, unlayered material—are prone to fail through a rotational sliding process (Hungr et al. 2014). Another type is reservoir landslides, which—caused by unbalanced groundwater levels due to lake water dynamics—tend to fail along a failure surface in a translational mode. Li et al. (2019) and Tang et al. (2019) extensively studied LTT in the Three Gorges Reservoir and concluded that most slopes fail because of sliding processes along bedding planes due to water level variations or rainfall. Paraglacial conditions caused many fall-type landslides, including rock falls in fjord environments and glacier calving events. The only toppling event in the database was caused by precipitation (Furnas Lake, Brazil, in 2022, Maciel et al. 2023; Fig. 1, no. 31). Since flank collapses are exclusively related to volcanic landslides, their only cause is volcanic activity. The same applies equivalently to coastal subsidence, a landslide type only reported in association with earthquakes.

The vast majority of mass movements have a large (63%) or medium (29%) volume and were caused in about equal proportions by the six different cause classes (Fig. 6d). The database contains only one case study (< 1%) of an LTT triggered by a landslide with a small volume of less than 1,000 m^3. Only a few tsunamis were triggered by giant (6%) and monster (< 1%) landslides. Those landslides with a volume exceeding 1 km^3 are caused by geologic processes such as earthquakes and volcanic activity. The only LTT triggered by a monster landslide is the well-known Storegga landslide and tsunami located offshore of Norway (Fig. 1). The landslide with a volume of about 3,200 km^3 caused tsunami waves, whose deposits are still visible at the coast of the entire North Sea and Northern Atlantic Ocean (Bondevik et al. 1997; Haflidason et al. 2004).

2.4.2 Generated water heights

Figure 7 shows the correlation between the landslide characteristics described above and the maximum water heights. The values range from very small, barely measurable waves of 0.06 m (Resurrection Bay, Alaska, 2022, National Geophysical Data Center 2024; Fig. 1, no. 41), and up to extremely high run-ups of 524 m in Lituya Bay, Alaska, in 1958 (Miller 1960). For each landslide characteristic, the maximum water height values exhibit considerable spread across parameter values, with a direct correlation between any single landslide characteristic and the maximum water height not obvious. As tsunami wave height is controlled by multiple variables—including landslide characteristics, water depth, and water body and coastal geometry (Pelinovsky and Mazova 1992; Fritz et al. 2004; Løvholt et al. 2015)—a direct correlation to only one of the influencing parameters is impossible. Furthermore, the maximum water height corresponds either to the maximum run-up height or the maximum wave height, depending on the data availability, with a considerable difference existing between these two values. Nevertheless, some correlations can be observed in Fig. 7.

Most extremely high waves larger than 100 m were triggered by subaerial landslides consisting of hard rock and occurred in inland waters or enclosed marine environments (Fig. 7a and b). As described in Sect. 2.3, tsunami energy and wave height dissipate slowly

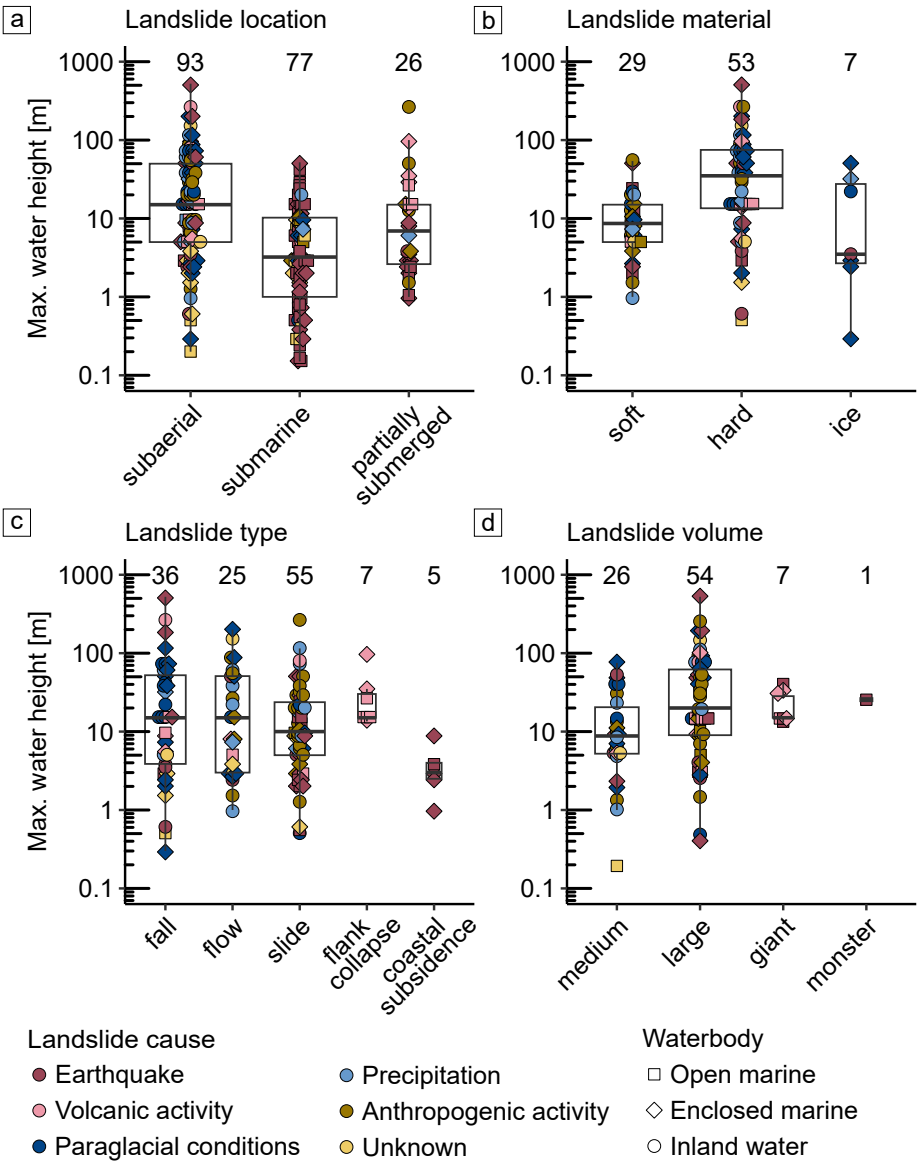

Fig. 7 Landslide parameters and their correlation with the maximum tsunami water height, defined as the larger value between the maximum run-up height and the maximum wave height: **a**) landslide location, **b**) landslide material, **c**) landslide type, and **d**) landslide volume. Numbers above each box plot indicate the number of observations per class

in inland waters and enclosed marine environments, allowing the formation of high waves (Couston et al. 2015; Fuchs and Hager 2015). In open marine environments, tsunamis with wave heights greater than 10 m were documented almost exclusively due to mass movements with giant or monster volumes (Fig. 7d). These giant and monster volumes provide large amounts of kinetic energy, which is required to generate high waves in open marine

environments, where coastlines or other morphological structures that could cause wave reflections are absent, and tsunami energy quickly attenuates before the waves reach the nearest shoreline. The highest wave in an open marine environment was recorded in 1946 during the Aleutian tsunami (Lander et al. 1993; Fig. 1, no. 32). With a height of 42 m, it is far smaller than the highest wave measured in inland waters, 260 m in Vajont, Italy (Barla and Paronuzzi 2013), or enclosed marine environments, 524 m in Lituya Bay, Alaska (Miller 1960).

Coseismic landslides triggered numerous small tsunamis with water heights below 1 m. Urgeles and Camerlenghi (2013) compiled data on submarine landslides in the Mediterranean Sea and found that landslides in active tectonic environments tend to occur more frequently than in passive tectonic settings, but are smaller and trigger smaller waves. Similar conclusions were drawn by Brink and Geist (2021) for landslides off the U.S. coasts and by Völker et al. (2011) off central Chile. Furthermore, coastal communities in active tectonic environments are often well-prepared for tsunamis and equipped with tide gauges. Thus, even tsunamis with small amplitudes can be detected and documented, whereas they might otherwise remain unnoticed.

Regarding landslide type, tsunamis triggered by coastal subsidence tend to generate smaller wave heights (< 10 m), while landslides associated with volcano flank collapses tend to produce larger waves (> 10 m, Fig. 7c). However, observations for both classes are very limited, so no reliable conclusions can be drawn.

Several studies, including Murty (2003) and Hughes et al. (2024), have investigated the correlation between landslide volume and tsunami wave height, observing a positive connection. However, the database shows that landslides with the highest volumes do not necessarily trigger the highest waves. Landslides with giant or monster volumes generated tsunamis with maximum water heights on the order of tens of meters, while the highest waves were triggered by large landslides (Fig. 7d). Notably, none of these giant or monster landslides occurred in inland waters—only in marine environments, where tsunami energy dissipates more rapidly. Such extremely large landslides were caused by two scenarios in the past: either failure of the sediments on the continental slope, typically far from the nearest shoreline, resulting in wave attenuation before reaching the coast (e.g., Storegga, 8200 BP, 3200 km³, Haflidason et al. 2004; Fig. 1), or collapse of a volcanic flank, documented only in open and enclosed marine environments (e.g., Krakatau, 1883, 12 km³, Nomanbhoy and Satake 1995).

Additional parameters are highly relevant for the development of maximum water height. For example, a landslide with a monster volume can slide at very low speed and thus induce only low wave heights. In particular, the location where the landslide occurs and the tsunami is triggered is of utmost importance for wave generation (Løvholt et al. 2020). Løvholt et al. (2015) reviewed parameters influencing wave generation, concluding that the frontal landslide area and impact velocity often characterize subaerial LTT. Submarine LTT are more influenced by the initial landslide acceleration for long run-out landslides or, for short run-out landslides, by the landslide Froude number Fr (defined as the ratio between landslide velocity u, landslide thickness d, and gravitational acceleration g: $Fr = u/\sqrt{gd}$). However, due to data scarcity, other parameters are not covered in this database.

3 Consequences

To investigate the consequences of LTT for coastal communities, the fatalities and economic damage resulting from LTT, their correlation with maximum water heights, and their spatial distribution are discussed. A genuine hazard analysis requires data reflecting the specific threat posed by an LTT at a given location and its return period. For risk analysis, data on the exposure of elements at risk and their vulnerability to LTT are additionally required alongside the temporal component (Fell et al. 2005). Since the number of documented LTT cases worldwide is limited and individual cases vary significantly—for example, in terms of location and wave height—it is difficult to determine return periods for a specific hazard. A full hazard or risk analysis is therefore not possible with the available data, but the parameters fatalities and damage allow assessment of LTT consequences without considering the total number of exposed elements at risk or their vulnerability.

Figure 8 displays the correlation between fatalities and tsunami damage resulting from historical LTT, allowing a detailed investigation of their causes and waterbodies. As data availability for tsunami damage is scarce, only a limited number of 110 LTT is therefore illustrated in Fig. 8.

Most LTT caused few fatalities (< 50) and minor damage (< 5×10^6 US$). They belong to all six cause classes and occur in all water bodies. LTT that caused a large number of fatalities (> 100) and severe damage (> 5×10^6 US$) were mainly induced by earthquakes and volcanic activity, occurring in open and enclosed marine environments (Fig. 8). Figure 9 shows that these LTT have large maximum water heights. Additionally, the database reveals that ten of these 18 LTT occurred in Southeast Asia—eight in Indonesia and two in Papua New Guinea (Dohmen et al. 2025). This is a region with a very high population density along the coastline, making the population particularly exposed to tsunamis. The only two

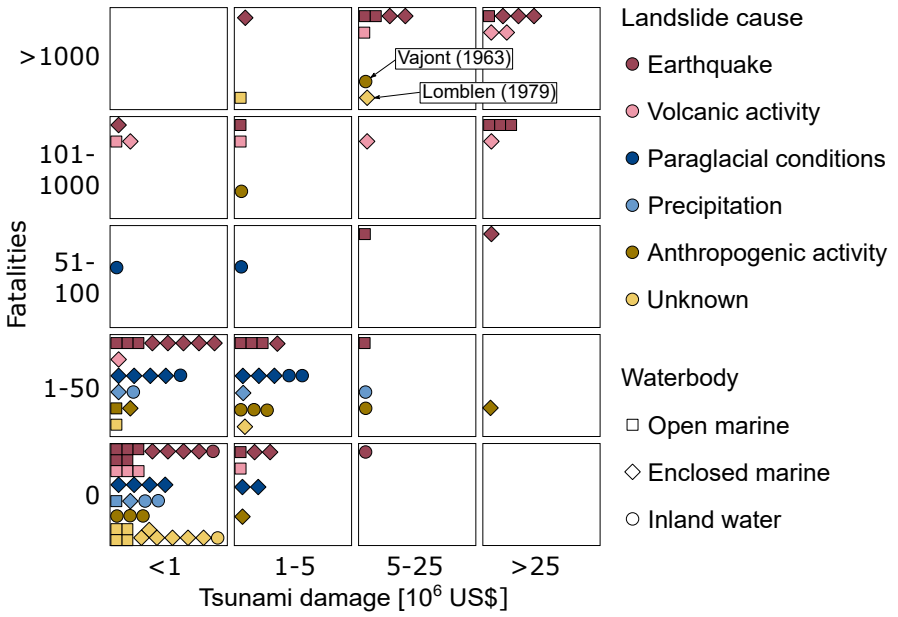

Fig. 8 Tsunami damage and fatalities resulting from LTT (total number = 110)

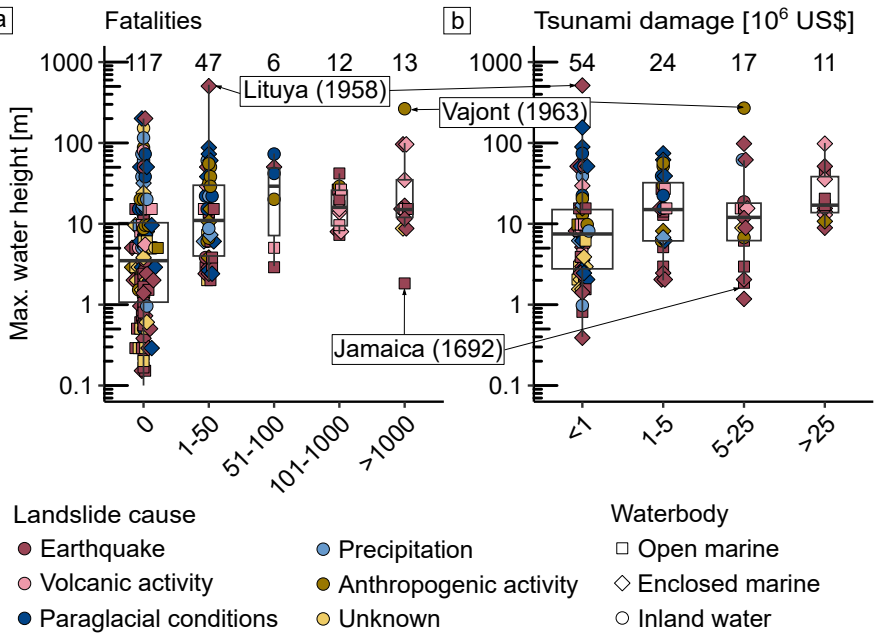

Fig. 9 Number of fatalities (**a**) and amount of tsunami damage (**b**) and their correlation with the maximum tsunami water height, defined as the larger value of the maximum run-up height and the maximum wave height. Numbers above each box plot represent the number of observations per class

LTT not related to seismic or volcanic activity that caused more than 100 fatalities and damage exceeding 5×10^6 US$ are the Vajont tsunami (Barla and Paronuzzi 2013) and another case in Lomblen, Indonesia, in 1979 (Soloviev and Go 1974; Fig. 1, no. 35).

Figure 9 displays the correlation between maximum water height and fatalities or tsunami damage. Most documented LTT did not cause any fatalities, even when generated waves reached heights of up to 200 m (Fig. 9a). It can be observed that rather high waves (> 5 m) caused many fatalities and large amounts of damage. However, water height values vary significantly within each fatality and damage class, indicating that high waves do not necessarily cause many fatalities or extensive damage. One reason is that the available data do not provide information on the exposure or vulnerability of people and infrastructure. For example, the LTT with the highest generated waves (524 m) caused only two casualties and 0.1×10^6 US$ in damage, as it occurred in a remote area in Alaska (Miller 1960). In contrast, small waves can have catastrophic consequences when affecting densely populated areas. For instance, in Port Royal, Jamaica, a wave of only 1.8 m hit the coastline in 1692, causing about 2,000 fatalities and considerable damage of $5–25 \times 10^6$ US$ (Lander et al. 2002; Fig. 1, no. 36).

Figure 10 reveals the distribution of fatalities and economic losses caused by LTT in different parts of the world. Countries such as the U.S. (dark blue) and Norway (light blue) are frequently affected by LTT (70 and 32 times, respectively; Fig. 10a). However, the number of fatalities from LTT is relatively low in both countries (362 and 250, respectively; Fig. 10b), as the waves often occur in remote areas with low population density. Neverthe-

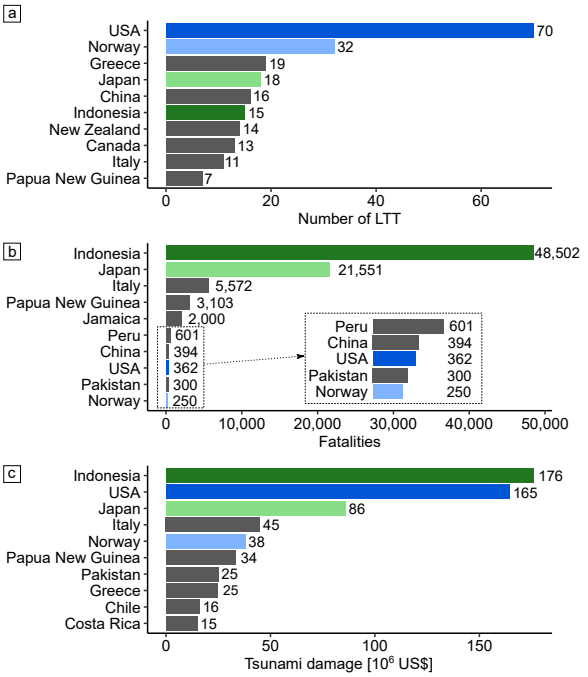

Fig. 10 Spatial distribution of (**a**) the number of LTT events, (**b**) the total fatalities, and (**c**) total tsunami damage per country for the ten countries with the highest values. Since tsunami damage data from the National Geophysical Data Center (2024) database are only available in classified form, a unique value was assigned to each class to calculate the total for each country. The following values were used: $<1 = 0.5 \times 10^6$ US$, 1–5 $= 2.5 \times 10^6$ US$, 5–25 $= 15 \times 10^6$ US$ and $>25 = 25 \times 10^6$ US$

less, considerable economic damage—165×10^6 US$ and 32×10^6 US$ in Norway—was caused to infrastructure in these highly developed countries (Fig. 10c).

In contrast, countries such as Indonesia (dark green) and Japan (light green) have a high death toll from LTT (Fig. 10b). The impacts in these countries are characterized by a small number of catastrophic LTT events causing an enormous number of fatalities. As mentioned earlier in this section, eight of the 18 deadliest and most damaging LTT occurred in Indonesia, including the 1883 Krakatau LTT (34,000 fatalities, Nomanbhoy and Satake 1995), the 1899 Seram LTT (3,864 fatalities, Rynn 2002; Fig. 1, no. 37), and the 1674 Ambon LTT (2,300 fatalities, Pranantyo and Cummins 2020; Fig. 1, no. 38). Some of the most destructive LTT in Japan include the tsunami following the Mt. Mayuyama flank collapse in 1792 (15,000 fatalities, Miyamoto 2010; Fig. 1, no. 25) and the tsunami caused by the eruption of the Oshima-Oshima volcano in 1741 (2,000 fatalities, Ioki et al. 2019; Fig. 1, no. 42). LTT in Indonesia and Japan were triggered almost entirely by earthquakes and volcanic activity. Both countries are located at the junction of several tectonic plates and a major subduction zone (Hamilton 1979; Taira 2001), resulting in high seismic and volcanic activity. Additionally, both countries consist of multiple islands, with large portions of their populations living in low-lying coastal areas, making them particularly vulnerable to LTT.

4 Implications for mitigation

The distribution of historical LTT shows that a large portion of worldwide coastlines, particularly along active continental margins, are affected by these events (Fig. 1). Examination of the LTT catalog demonstrates that they are highly complex phenomena. The maximum

water height is influenced by the triggering mass movement, which can vary widely in characteristics. The volumes of documented mass movements span up to 10 orders of magnitude (Fig. 6), while whether the landslide occurs subaerially or underwater is another critical factor. Other important parameters influencing wave generation, such as the initial speed and acceleration of landslides (Løvholt et al. 2015), are not addressed in this review due to limited data availability. Additionally, the geometry of the water body and coastline plays a crucial role in determining wave heights at the shore. Given the complexity of LTT and the multitude of influencing factors, predicting wave heights based on the 317 studied cases is currently impossible. Because of the widespread probability of occurrence and the unpredictability of wave heights, implementing structural risk reduction measures such as tsunami protective walls or slope stabilization remains ineffective to date. However, this study aims to reduce uncertainty surrounding LTT by narrowing down areas at increased risk and characterizing cases that pose a high threat to communities. Analysis of the LTT catalog reveals some correlations in the spatial distribution, size, and causes of LTT, which could inform improved risk mitigation strategies and early warning systems.

In general, the highest waves were generated in inland waters and enclosed marine environments (Fig. 7). These local tsunamis are characterized by short propagation distances and limited warning times. Early warning is only feasible in exceptional cases, when an unstable slope is known and landslide monitoring is possible. In such instances, landslide monitoring and early warning systems can provide tsunami alerts by detecting slope instability before wave generation. An example is the LTT early warning system in Tafjord, Norway, where an unstable slope of up to 54×10^6 m³ is continuously monitored using various sensors. If slope failure is imminent, the local population is warned via cell phone alerts, sirens, and media channels, then evacuated before the event (Åknes / Tafjord Emergency Response Team 2025). Similarly, many reservoir landslide monitoring and early warning systems exist in China (e.g., Wushan town, Yin et al. 2010; Longmen, Wang et al. 2024; Outang, Wang et al. 2021a). Yin et al. (2010) report that 3,200 landslides within the Three Gorges Reservoir area are monitored. However, these systems focus solely on landslide detection and do not directly address the probability of displacement waves. Therefore, landslide monitoring should be integrated with tsunami early warning systems and evacuation planning to effectively protect coastal populations and ensure safe navigation. For most tsunamigenic landslides, however, the precise location is unknown beforehand, making proactive monitoring impractical. In such cases, hazard and risk reduction rely primarily on public awareness and education to encourage self-evacuation.

LTT are strongly associated with earthquakes, which are the most frequent cause of LTT (Fig. 5), with earthquake-induced LTT causing the highest fatalities and damages historically (Figs. 8 and 9). Established seismic tsunami early warning systems, such as the Indonesia Tsunami Early Warning System (InaTEWS; https://inatews.bmkg.go.id/), provide reliable warnings to the population. InaTEWS uses a dual early warning system approach, combining the finite element model TsunAWI and the linear long-wave model easyWave to estimate wave height (EWH) and time of arrival (ETA) (Harig et al. 2020). However, tsunamis generated by coseismic landslides can produce higher waves or arrive sooner at the coastline than those triggered directly by the earthquake, as observed in Palu Bay (Carvajal et al. 2019; Omira et al. 2019). Therefore, in addition to standard warnings of wave height and arrival time, existing tsunami early warning systems should also issue alerts for exceptionally high waves caused by submarine landslides that may arrive immediately after

the earthquake. Du et al. (2025) recently demonstrated that coseismic submarine landslides predominantly occur during earthquakes on strike-slip faults. Consequently, this additional warning is particularly important for regions near large active strike-slip fault zones, such as Palu Bay in Indonesia and the Izmit Bay at the edge of the Sea of Marmara, Turkey, where coseismic landslides during the 1999 Kocaeli earthquake triggered 3 m high waves (Altinok et al. 2001; Fig. 1, no. 39).

Large LTT can have ocean-wide impacts, threatening coastlines hundreds or even thousands of kilometers from the triggering landslide. For example, the 1929 Grand Banks tsunami, triggered offshore in the Atlantic Ocean near Canada, was recorded as far away as Portugal (Fine et al. 2005). Such tsunamis can be detected and reported by DART (Deep-ocean Assessment and Reporting of Tsunamis) buoys, which are integral components of modern tsunami early warning systems (Gonzalez et al. 1998).

Several approaches exist for establishing volcanic tsunami early warning systems or integrating warnings for landslide-triggered waves into existing tsunami early warning frameworks, for example, at Stromboli, Hawaii, Hunga Tonga, Anak Krakatau, and in the Caribbean (Schindelé et al. 2024). Given the diverse and complex triggering mechanisms of volcanic tsunamis, these systems primarily rely on sea level measurements near the volcanoes and are closely linked to volcano observatories (Schindelé et al. 2024). Such systems detect all types of volcanic tsunamis, including volcanic LTT, and are therefore generally suitable for detecting various LTT. Some of the deadliest historical LTT—such as those at Krakatau in 1883 and 2018, Mount Mayuyama in 1792, and Oshima-Oshima in 1741—caused significant damage and fatalities at locations both near and far from the landslide epicenter. Consequently, early warning systems for volcanic tsunamis can play a crucial role in hazard management by enabling evacuation even in areas far from the source, where longer warning times are possible.

Most landslides that trigger tsunamis have volumes smaller than one cubic kilometer (Fig. 6) and therefore cannot be resolved by publicly available low-resolution bathymetry datasets, such as the General Bathymetric Chart of the Oceans (GEBCO), which has a spatial resolution of 15 arc-seconds (GEBCO Bathymetric Compilation Group). Consequently, more high-resolution bathymetry data are essential to detect and study tsunamigenic submarine landslides. Investigating their spatial distribution, magnitude-frequency relationships, and failure mechanisms is critical for advancing the understanding and improving predictions of future events. Data acquisition efforts could follow examples like the Italian MaGIC (Marine Geohazards along the Italian Coasts) program, which systematically acquires high-resolution multibeam bathymetry data covering extensive portions of the Italian coastline (Chiocci and Ridente 2011). Additionally, detecting landslides through seismic monitoring, as demonstrated by Lin et al. (2010) for landslides triggered by Typhoon Morakot in Taiwan, or by Vera et al. (2025) for the Krakatau volcano collapse in Indonesia, represents a promising complementary approach. Integrating these seismic detections with sea level measurements can enhance our understanding of the spatial and temporal occurrence of landslides and the tsunamis they generate.

5 Conclusions

Based on a catalog of 317 LTT, this review examines their spatial distribution, triggering causes, and landslide characteristics, correlating these factors with the resulting wave heights and local impacts. The catalog identifies seismic and volcanic activity as the primary triggers for tsunamigenic landslides that pose the greatest threat to coastal communities. Consequently, coastlines along active tectonic margins—such as those in Indonesia, Japan, and the U.S.—are the most affected globally by LTT. Indonesia, with nearly 50,000 fatalities and $176 million in damage, is the most severely impacted country, followed by Japan (21,000 fatalities, $86 million in damage). In contrast, countries like the U.S. and Norway experience numerous LTT events but comparatively few fatalities and moderate economic losses. The largest waves tend to be generated in inland waters and enclosed marine environments, with LTT in inland waters mainly caused by anthropogenic activities, particularly in reservoir lakes. Effective early warning systems for LTT require continuous monitoring of landslide activity, sea levels near the landslide source, and access to high-resolution multibeam bathymetry data. However, precise knowledge of landslide locations is necessary—something generally available only for active volcanoes and a limited number of subaerial landslides, especially in water reservoirs.

A major challenge in the study of LTT is the limited availability of data, particularly from submarine environments. Key parameters that influence the generation and propagation of LTT—such as landslide velocity—are not captured in this catalog. Moreover, submarine LTT are likely underrepresented, as only those events that produce coastal waves are typically documented. To reduce future risks from LTT in coastal regions, the ability to identify and predict potential events is essential. Landslide susceptibility mapping, which is widely used in subaerial settings (e.g., Reichenbach et al. 2018), is a promising tool for this purpose. In addition, high-resolution bathymetry data can help detect smaller landslides—responsible for the majority of LTT—and delineate areas with morphological features indicative of failure potential. In regions where potentially tsunamigenic landslides have already been identified, such as in many reservoir lakes, risk reduction measures should include inundation mapping, development of evacuation plans, the implementation of early warning systems, and public education on LTT-related hazards.

Author contributions All authors contributed to the study's conception and design. Data collection was performed by Katrin Dohmen. All authors contributed to the data analysis. The first draft of the manuscript was written by Katrin Dohmen and all authors reviewed and edited previous versions of the manuscript. All authors read and approved the final manuscript.

Funding Open Access funding enabled and organized by Projekt DEAL. This research was supported by the Federal Ministry of Education and Research of Germany in the framework of the TSUNAMI_RISK project (grant no. 03G0906E), which is a part of the funding initiative CLIENT-II.

Code and data availability The LTT database is published in the PANGAEA repository (Dohmen et al. 2025).

Declarations

Competing interests The authors have no relevant financial or non-financial interests to disclose.

References

Aarseth I, Lønne Ø, Giskeødegaard O (1989) Submarine slides in glaciomarine sediments in some Western Norwegian Fjords. Mar Geol 88:1–21. https://doi.org/10.1016/0025-3227(89)90002-9

Åknes / Tafjord Emergency Response Team (2025) https://www.aknes.no/. Accessed 22 January 2025

Alberico I, Budillon F, Casalbore D, Di Fiore V, Iavarone R (2018) A critical review of potential tsunamigenic sources as first step towards the tsunami hazard assessment for the Napoli Gulf (Southern Italy) highly populated area. Nat Hazards 92:43–76. https://doi.org/10.1007/s11069-018-3191-5

Altinok Y, Tinti S, Alpar B, Yalçiner AC, Ersoy Ş, Bortolucci E, Armigliato A (2001) The tsunami of August 17, 1999 in Izmit bay, Turkey. Nat Hazards 24:133–146. https://doi.org/10.1023/A:1011863610289

Aránguiz R, Caamaño D, Espinoza M, Gómez M, Maldonado F, Sepúlveda V, Rogel I, Oyarzun JC, Duhart P (2023) Analysis of the cascading rainfall–landslide–tsunami event of June 29th, 2022, Todos Los Santos lake. Chile Landslides 20:801–811. https://doi.org/10.1007/s10346-022-02015-1

Arikawa T, Muhari A, Okumura Y, Dohi Y, Afriyanto B, Sujatmiko KA, Imamura F (2018) Coastal subsidence induced several tsunamis during the 2018 Sulawesi earthquake. J Disaster Res 13:sc20181201. https://doi.org/10.20965/jdr.2018.sc20181201

Assier-Rzadkieaicz S, Heinrich P, Sabatier PC, Savoye B, Bourillet JF (2000) Numerical modelling of a landslide-generated tsunami: the 1979 nice event. Pure Appl Geophys 157:1707–1727. https://doi.org/10.1007/PL00001057

Ballantyne CK (2002) Paraglacial geomorphology. Quat Sci Rev 21:1935–2017. https://doi.org/10.1016/S0277-3791(02)00005-7

Barla G, Paronuzzi P (2013) The 1963 Vajont landslide: 50th anniversary. Rock Mech Rock Eng 46:1267–1270. https://doi.org/10.1007/s00603-013-0483-7

Benz SA, Blum P (2019) Global detection of rainfall-triggered landslide clusters. Nat Hazards Earth Syst Sci 19:1433–1444. https://doi.org/10.5194/nhess-19-1433-2019

Blais-Stevens A, Geertsema M, Schwab JW, Bornhold BD, Mosher D (2006) A brief overview of landslide-generated tsunamis affecting North America

Bondevik S, Sevendsen JI, Mangerud JA (1997) Tsunami sedimentary facies deposited by the Storegga tsunami in shallow marine basins and coastal lakes, Western Norway. Sedimentology 44:1115–1131. https://doi.org/10.1046/j.1365-3091.1997.d01-63.x

Brideau M-A, Sturzenegger M, Stead D, Jaboyedoff M, Lawrence M, Roberts NJ, Ward BC, Millard TH, Clague JJ (2012) Stability analysis of the 2007 chehalis lake landslide based on long-range terrestrial photogrammetry and airborne lidar data. Landslides 9:75–91. https://doi.org/10.1007/s10346-011-0286-4

Brunner FK, Scheidegger AE (1973) Exfoliation Rock Mech 5:43–62. https://doi.org/10.1007/BF01246756

Caine N (1982) Toppling failures from alpine cliffs on Ben lomond, Tasmania. Earth Surf Proc Land 7:133–152. https://doi.org/10.1002/esp.3290070207

Carrillo-Ponce A, Heimann S, Petersen GM, Walter TR, Cesca S, Dahm T (2024) The 16 September 2023 Greenland megatsunami: analysis and modeling of the source and a week-long, monochromatic seismic signal. Seism Rec 4:172–183. https://doi.org/10.1785/0320240013

Carvajal M, Araya-Cornejo C, Sepúlveda I, Melnick D, Haase JS (2019) Nearly instantaneous tsunamis following the Mw 7.5 2018 palu earthquake. Geophys Res Lett 46:5117–5126. https://doi.org/10.1029/2019GL082578

Casalbore D, Romagnoli C, Bosman A, Chiocci FL (2011) Potential tsunamigenic landslides at stromboli volcano (Italy): insight from marine DEM analysis. Geomorphology 126:42–50. https://doi.org/10.1016/j.geomorph.2010.10.026

Chen S, Shi A, Xu W, Yan L, Wang H, Tian L, Xie W-C (2023) Numerical investigation of landslide-induced waves: a case study of Wangjiashan landslide in Baihetan reservoir, China. Bull Eng Geol Environ 82. https://doi.org/10.1007/s10064-023-03148-w

Chen S, Xu W, Zhang G, Wang R, Yan L, Zhang H, Wang H (2024) Numerical simulation of potential impulse waves generated by the Mogu rock landslide at varying water levels in the Lianghekou reservoir, China. Landslides 21:2289–2305. https://doi.org/10.1007/s10346-024-02286-w

Chiocci FL, Ridente D (2011) Regional-scale seafloor mapping and geohazard assessment. The experience from the Italian project magic (Marine geohazards along the Italian Coasts). Mar Geophys Res 32:13–23. https://doi.org/10.1007/s11001-011-9120-6

Clare MA, Hughes Clarke JE, Talling PJ, Cartigny M, Pratomo DG (2016) Preconditioning and triggering of offshore slope failures and turbidity currents revealed by most detailed monitoring yet at a fjord-head delta. Earth Planet Sci Lett 450:208–220. https://doi.org/10.1016/j.epsl.2016.06.021

Clostermann M (2013) Report on the determination of the causes of the Nachterstedt embankment movement in Saxony-Anhalt: Executive summary. (in German language). https://mwl.sachsen-anhalt.de/fileadmin/Bibliothek/Politik_und_Verwaltung/MW/Bergbau/Clostermann-Zusammenfassung.pdf. Accessed 9 August 2023

Corsa BD, Jacquemart M, Willis MJ, Tiampo KF (2022) Characterization of large tsunamigenic landslides and their effects using digital surface models: A case study from Taan fiord, Alaska. Remote Sens Environ 270:112881. https://doi.org/10.1016/j.rse.2021.112881

Coulter HW, Migliaccio RR (1966) Effects of the earthquake of March 27, 1964, at valdez, Alaska. https://doi.org/10.3133/pp542c. USGS Professional Paper

Couston L-A, Mei CC, Alam M-R (2015) Landslide tsunamis in lakes. J Fluid Mech 772:784–804. https://doi.org/10.1017/jfm.2015.190

Crosta GB, Imposimato S, Roddeman D (2016) Landslide spreading, impulse water waves and modelling of the Vajont rockslide. Rock Mech Rock Eng 49:2413–2436. https://doi.org/10.1007/s00603-015-0769-z

Dahl-Jensen T, Larsen LM, Pedersen SAS, Pedersen J, Jepsen HF, Pedersen G, Nielsen T, Pedersen AK, von Platen-Hallermund F, Weng W (2004) Landslide and tsunami 21 November 2000 in paatuut, West Greenland. Nat Hazards 31:277–287. https://doi.org/10.1023/B:NHAZ.0000020264.70048.95

Davies MCR, Hamza O, Harris C (2001) The effect of rise in mean annual temperature on the stability of rock slopes containing ice-filled discontinuities. Permafr Periglac Process 12:137–144. https://doi.org/10.1002/ppp.378

Di Traglia F, Fornaciai A, Casalbore D, Favalli M, Manzella I, Romagnoli C, Chiocci FL, Cole P, Nolesini T, Casagli N (2022) Subaerial-submarine morphological changes at stromboli volcano (Italy) induced by the 2019–2020 eruptive activity. Geomorphology 400:108093. https://doi.org/10.1016/j.geomorph.2021.108093

Di Traglia F, Berardino P, Borselli L, Calabria P, Calvari S, Casalbore D, Casagli N, Casu F, Chiocci FL, Civico R, de Cesare W, de, Del Soldato LC, Esposito M, Esposito A, Favalli C, Fornaciai M, Giudicepietro A, Gracchi F, Lanari T, Macedonio R, Monterroso G, Natale F, Nolesini A, Perna T, Ricci S, Romagnoli T, Rossi C, Stefanelli G CT (2024) Generation of deposit-derived pyroclastic density currents by repeated crater rim failures at stromboli volcano (Italy). Bull Volcanol 86. https://doi.org/10.1007/s00445-024-01761-5

Dirección General del Instituto Geográfico Nacional (2023) Catálogo de tsunamis En Las Costas Españolas. Centro Nacional de Información Geográfica (Ministerio de Transportes. Movilidad y Agenda Urbana)

Dohmen K, Braun A, Fernandez-Steeger T (2025) A catalog of landslide-triggered tsunamis [dataset]. https://doi.org/10.1594/PANGAEA.979839. PANGAEA repository

Downes G, Barberopoulou A, Cochran U, Clark K, Scheele F (2017) The new Zealand tsunami database: historical and modern records. Seismol Res Lett 88:342–353. https://doi.org/10.1785/0220160135

Du P, Li L, Kopf A, Wang D, Chen K, Shi H, Wang W, Pan X, Hu G, Zhang P (2025) Earthquake-induced submarine landslides (EQISLs) and a comparison with their terrestrial counterparts: insights from a new database. Earth-Sci Rev 261:105021. https://doi.org/10.1016/j.earscirev.2024.105021

Duc DM, Khang DQ, Duc DM, Ngoc DM, Quynh DT, Thuy DT, Giang NKH, van Tien P, Ha NH (2020) Analysis and modeling of a landslide-induced tsunami-like wave across the truong river in Quang Nam Province. Vietnam Landslides 17:2329–2341. https://doi.org/10.1007/s10346-020-01434-2

Evans SG (1989) The 1946 Mount colonel foster rock avalanche and associated displacement wave, Vancouver island, British Columbia. Can Geotech J 26:447–452. https://doi.org/10.1139/t89-057

Fahmi MN, Realita A, Madlazim (2022) Rupture kinematic process of the Mw 5.9 Seram earthquake imaged by back-projection technique followed by the tsunami. Sci Tsunami Hazards 41:370–382

Fan X, Scaringi G, Korup O, West AJ, van Westen CJ, Tanyas H, Hovius N, Hales TC, Jibson RW, Allstadt KE, Zhang L, Evans SG, Xu C, Li G, Pei X, Xu Q, Huang R (2019) Earthquake-induced chains of geologic hazards: patterns, mechanisms, and impacts. Rev Geophys 57:421–503. https://doi.org/10.1029/2018RG000626

Fell R, Ho KKS, Lacasse S, Leroi E (2005) A framework for landslide risk assessment and management. In: Hungr O, Fell R, Couture EE (eds) Landslide risk management: Proceedings of the International Conference on Landslide Risk Management, Vancouver, Canada, 31 May-3 June 2005. A.A. Balkema Publishers, Leiden

Ferrer M, González-de-Vallejo LI (2024) Global historical megatsunamis catalog (GHMCat). GeoHazards 5:971–1017. https://doi.org/10.3390/geohazards5030048

Fine IV, Rabinovich AB, Bornhold BD, Thomson RE, Kulikov EA (2005) The grand banks landslide-generated tsunami of November 18, 1929: preliminary analysis and numerical modeling. Mar Geol 215:45–57. https://doi.org/10.1016/j.margeo.2004.11.007

Fjeldskaar W, Lindholm C, Dehls JF, Fjeldskaar I (2000) Postglacial uplift, neotectonics and seismicity in Fennoscandia. Quat Sci Rev 19:1413–1422. https://doi.org/10.1016/S0277-3791(00)00070-6

Forbes DL, Syvitski J (2010) Paraglacial Coasts. In: Carter RWG, Woodroffe CD, van Plassche O (eds) Coastal evolution. Cambridge University Press, pp 373–424. https://doi.org/10.1017/CBO9780511564420.012

Fritz HM, Hager WH, Minor H-E (2004) Near field characteristics of landslide generated impulse waves. J Waterw Port Coast Ocean Eng 130:287–302. https://doi.org/10.1061/(ASCE)0733-950X(2004)130:6(287)

Fritz HM, Kongko W, Moore A, McAdoo B, Goff J, Harbitz CB, Uslu B, Kalligeris N, Suteja D, Kalsum K, Titov VV, Gusman AR, Latief H, Santoso E, Sujoko S, Djulkarnaen D, Sunendar H, Synolakis CE (2007) Extreme runup from the 17 July 2006 Java tsunami. Geophys Res Lett 34:L24308. https://doi.org/10.1029/2007GL029404

Fuchs H, Hager WH (2015) Solitary impulse wave transformation to overland flow. J Waterw Port Coast Ocean Eng 141. https://doi.org/10.1061/(ASCE)WW.1943-5460.0000294

Gamboa D, Omira R, Terrinha P (2021) A database of submarine landslides offshore West and Southwest Iberia. Sci Data 8:185. https://doi.org/10.1038/s41597-021-00969-w

Gariano SL, Guzzetti F (2016) Landslides in a changing climate. Earth-Sci Rev 162:227–252. https://doi.org/10.1016/j.earscirev.2016.08.011

Gauthier D, Anderson SA, Fritz HM, Giachetti T (2018) Karrat Fjord (Greenland) tsunamigenic landslide of 17 June 2017: initial 3D observations. Landslides 15:327–332. https://doi.org/10.1007/s10346-017-0926-4

GEBCO Bathymetric Compilation Group (2024) The GEBCO_2024 Grid - a continuous terrain model of the global oceans and land. https://doi.org/10.5285/1c44ce99-0a0d-5f4f-e063-7086abc0ea0f

Girardclos S, Schmidt OT, Sturm M, Ariztegui D, Pugin A, Anselmetti FS (2007) The 1996 AD delta collapse and large turbidite in lake Brienz. Mar Geol 241:137–154. https://doi.org/10.1016/j.margeo.2007.03.011

Gonzalez FI, Milburn HM, Bernard EN, Newman JC (1998) Deep-ocean assessment and reporting of tsunamis (DART®): Brief Overview and Status Report. Proceedings of the International Workshop on Tsunami Disaster Mitigation 19–22 January 1998, Tokyo, Japan

Götz A, Siebert M (2020) The slope movement of 18.07.2009 - Need for action by the LMBV in preparation of securing and remediation measures. (in German language). In: Lausitzer und Mitteldeutsche Bergbau-Verwaltungsgesellschaft (ed) The rehabilitation of the Nachterstedt opencast mine after the embankment movement of 2009. (in German language), Leipzig, pp 10–24

Grilli ST, Tappin DR, Carey S, Watt SFL, Ward SN, Grilli AR, Engwell SL, Zhang C, Kirby JT, Schambach L, Muin M (2019) Modelling of the tsunami from the December 22, 2018 lateral collapse of Anak Krakatau volcano in the Sunda Straits. Indonesia Sci Rep 9:11946. https://doi.org/10.1038/s41598-019-48327-6

Gusiakov VK, Makhinov AN (2021) December 11, 2018 landslide and 90-m icy tsunami in the Bureya water reservoir. https://doi.org/10.1007/978-3-030-60196-6_25. In: Sassa K, Mikoš M, Sassa S, Bobrowsky PT, Takara K, Dang K (eds) Understanding and reducing landslide disaster risk: Volume 1 - Sendai Landslide partnerships and Kyoto Landslide Commitment. Springer International Publishing, Cham, pp 351–360

Hack R, Alkema D, Kruse GA, Leenders N, Luzi L (2007) Influence of earthquakes on the stability of slopes. Eng Geol 91:4–15. https://doi.org/10.1016/j.enggeo.2006.12.016

Haflidason H, Sejrup HP, Nygård A, Mienert J, Bryn P, Lien R, Forsberg CF, Berg K, Masson D (2004) The Storegga slide: architecture, geometry and slide development. Mar Geol 213:201–234. https://doi.org/10.1016/j.margeo.2004.10.007

Hamilton WB (1979) Tectonics of the Indonesian region. USGS Prof Paper. https://doi.org/10.3133/pp1078

Harbitz CB, Pedersen G, Gjevik B (1993) Numerical simulations of large water waves due to landslides. J Hydraul Eng 119:1325–1342. https://doi.org/10.1061/(ASCE)0733-9429(1993)119:12(1325)

Harbitz CB, Løvholt F, Bungum H (2014) Submarine landslide tsunamis: how extreme and how likely? Nat Hazards 72:1341–1374. https://doi.org/10.1007/s11069-013-0681-3

Harig S, Immerz A, Weniza, Griffin J, Weber B, Babeyko A, Rakowsky N, Hartanto D, Nurokhim A, Handayani T, Weber R (2020) The tsunami scenario database of the Indonesia tsunami early warning system (InaTEWS): evolution of the coverage and the involved modeling approaches. Pure Appl Geophys 177:1379–1401. https://doi.org/10.1007/s00024-019-02305-1

Harris R, Major J (2017) Waves of destruction in the East indies: the Wichmann catalogue of earthquakes and tsunami in the Indonesian region from 1538 to 1877. Geol Soc Spec Publ 441:9–46. https://doi.org/10.1144/SP441.2

Heidarzadeh M, Gusman AR, Patria A, Widyantoro BT (2022) Potential landslide origin of the Seram Island tsunami in Eastern Indonesia on 16 June 2021 following an Mw 5.9 aarthquake. Bull Seismol Soc Am 112:2487–2498. https://doi.org/10.1785/0120210274

Heidarzadeh M, Miyazaki H, Ishibe T, Takagi H, Sabeti R (2023) Field surveys of September 2018 landslide-generated waves in the Apporo dam reservoir, japan: combined hazard from the concurrent occurrences of a typhoon and an earthquake. Landslides 20:143–156. https://doi.org/10.1007/s10346-022-01959-8

Heinrich P, Piatanesi A, Hébert H (2001) Numerical modelling of tsunami generation and propagation from submarine slumps: the 1998 Papua new Guinea event. Geophys J Int 145:97–111. https://doi.org/10.1111/j.1365-246X.2001.00336.x

Hermanns RL, Blikra LH, Naumann M, Nilsen B, Panthi KK, Stromeyer D, Longva O (2006) Examples of multiple rock-slope collapses from Köfels (Ötz valley, Austria) and Western Norway. Eng Geol 83:94–108. https://doi.org/10.1016/j.enggeo.2005.06.026

Hermanns RL, Oppikofer T, Roberts NJ, Sandøy G (2014) Catalogue of historical displacement waves and landslide-triggered tsunamis in Norway. In: Lollino G, Manconi A, Locat J, Huang Y, Canals Artigas M (eds) Engineering geology for society and territory - volume 4: marine and coastal processes. Springer International Publishing, Cham, s.l., pp 63–66

Huang B, Wang SC, Zhao YB (2017) Impulse waves in reservoirs generated by landslides into shallow water. Coast Eng 123:52–61. https://doi.org/10.1016/j.coastaleng.2017.03.003

Huang B, Yin Y, Tan J (2019) Risk assessment for landslide-induced impulse waves in the three Gorges reservoir, China. Landslides 16:585–596. https://doi.org/10.1007/s10346-018-1115-9

Hughes KE, Fitzsimons SJ, Howarth JD (2024) Lacustrine mass movements in active tectonic settings: lake tsunami sources in new zealand's South Island. Geomorphology 464:109359. https://doi.org/10.1016/j.geomorph.2024.109359

Hungr O, Fell R, Couture EE (eds) (2005) Landslide risk management: Proceedings of the International Conference on Landslide Risk Management, Vancouver, Canada, 31 May-3 June 2005. A.A. Balkema Publishers, Leiden

Hungr O, Leroueil S, Picarelli L (2014) The Varnes classification of landslide types, an update. Landslides 11:167–194. https://doi.org/10.1007/s10346-013-0436-y

Iida K, Cox DC, Pararas-Carayannis G (1967) Preliminary catalog of tsunami occurring in the Pacific ocean. HIG Data Report

Intergovernmental Oceanographic Commission (2019) Tsunami glossary. Fourth Ed IOC Technical Series, IOC/2008/TS/85 rev4. UNESCO, Paris

Ioki K, Tanioka Y, Yanagisawa H, Kawakami G (2019) Numerical simulation of the landslide and tsunami due to the 1741 Oshima-Oshima eruption in Hokkaido. Japan J Geophys Res Solid Earth 124:1991–2002. https://doi.org/10.1029/2018JB016166

Ioualalen M, Migeon S, Sardoux O (2010) Landslide tsunami vulnerability in the Ligurian sea: case study of the 1979 October 16 nice international airport submarine landslide and of identified geological mass failures. Geophys J Int 166:213. https://doi.org/10.1111/j.1365-246X.2010.04572.x

Jones FO, Embody DR, Peterson WL (1961) Landslides along the Columbia river valley, Northeastern washington: descriptions of landslides and statistical analyses of data on some 2OO landslides in pleistocene sediments. USGS Professional Paper, vol 367. U.S. Government Printing Office

Katzenbach R, Werner A, Fischer S (2013) Methodology and result of the root cause analysis/investigation measures. (in German language). In: Report on the determination of the causes of the Nachterstedt embankment movement in Saxony-Anhalt: Executive summary. (in German language), pp 25–34

Keating BH, McGuire WJ (2000) Island edifice failures and associated tsunami hazards. Pure Appl Geophys 157:899–955. https://doi.org/10.1007/s000240050011

Keefer DK (2002) Investigating landslides caused by earthquakes – a historical review. Surv Geophys 23:473–510. https://doi.org/10.1023/A:1021274710840

Keefer DK (1984) Landslides caused by earthquakes. 1943–2674 95:406–421. https://doi.org/10.1130/0016-7606(1984)95%3C;406:LCBE%3E;2.0.CO;2

Keqiang H, Xiangran L, Xueqing Y, Dong G (2008) The landslides in the three Gorges reservoir region, China and the effects of water storage and rain on their stability. Environ Geol 55:55–63. https://doi.org/10.1007/s00254-007-0964-7

Keqiang H, Shangqing W, Du Wen, Sijing W (2010) Dynamic features and effects of rainfall on landslides in the three Gorges reservoir region, china: using the Xintan landslide and the large Huangya landslide as the examples. Environ Earth Sci 59:1267–1274. https://doi.org/10.1007/s12665-009-0114-5

Kim J, Coe JA, Lu Z, Avdievitch NN, Hults CP (2022) Spaceborne InSAR mapping of landslides and subsidence in rapidly deglaciating terrain, glacier Bay National park and preserve and vicinity, Alaska and British Columbia. Remote Sens Environ 281:113231. https://doi.org/10.1016/j.rse.2022.113231

Kirby JT, Shi F, Nicolsky D, Misra S (2016) The 27 April 1975 kitimat, British columbia, submarine landslide tsunami: a comparison of modeling approaches. Landslides 13:1421–1434. https://doi.org/10.1007/s10346-016-0682-x

Kirschbaum D, Adler R, Adler D, Peters-Lidard C, Huffman G (2012) Global distribution of extreme precipitation and high-impact landslides in 2010 relative to previous years. J Hydrometeorol 13:1536–1551. https://doi.org/10.1175/JHM-D-12-02.1

Kostrzewa O, Szczypińska M, Kavan J, Senderak K, Novák M, Strzelecki MC (2024) A boulder beach formed by waves from a calving glacier revisited: multidecadal tsunami–controlled coastal changes in front of eqip sermia, West Greenland. Permafr Periglac Process 35:312–325. https://doi.org/10.1002/ppp.2235

Krastel S, Behrmann JH, Völker D, Stipp M, Berndt C, Urgeles R, Chaytor JD, Huhn K, Strasser M, Harbitz CB (eds) (2014) Submarine mass movements and their consequences: 6th International Symposium. Advances in natural and technological hazards research, vol 37. Springer, Cham

Kremer K, Simpson G, Girardclos S (2012) Giant lake Geneva tsunami in AD 563. Nat Geosci 5:756–757. https://doi.org/10.1038/ngeo1618

Kremer K, Anselmetti FS, Evers FM, Goff J, Nigg V (2021) Freshwater (paleo)tsunamis – a review. Earth-Sci Rev 212:103447. https://doi.org/10.1016/j.earscirev.2020.103447

L'Heureux J-S, Eilertsen RS, Glimsdal S, Issler D, Solberg I-L, Harbitz CB (2012) The 1978 quick clay landslide at Rissa, Mid Norway: subaqueous morphology and tsunami simulations. In: Yamada Y, Kawamura K, Ikehara K, Ogawa Y, Urgeles R, Mosher D, Chaytor JD, Strasser M (eds) Submarine mass movements and their consequences: 5th International Symposium. Springer Science+Business Media B.V, Dordrecht, pp 507–516

L'Heureux J-S, Longva O, Hansen L, Vanneste M (2014) The 1930 landslide in Orkdalsfjorden: morphology and failure mechanism. https://doi.org/10.1007/978-3-319-00972-8_21. In: Krastel S, Behrmann JH, Völker D, Stipp M, Berndt C, Urgeles R, Chaytor JD, Huhn K, Strasser M, Harbitz CB (eds) Submarine mass movements and their consequences: 6th International Symposium, vol 37. Springer, Cham, pp 239–247

Lander JF (1997) Tsunamis affecting alaska, 1737–1996. NGDC key to geophysical research Documentation, vol 31. National Geophysical Data Center, Boulder, Colorado, USA

Lander JF, Lockridge PA, Kozuch MJ (1993) Tsunamis affecting the West Coast of the united states, 1806–1992. NGDC key to geophysical records Documentation, vol 29. National Geophysical Data Center, Boulder, Colorado, USA

Lander JF, Whiteside LS, Lockridge PA (2002) A brief history of tsunamis in the Caribbean sea. Sci Tsunami Hazards 20:57–94

Lander JF, Whiteside LS, Lockridge PA (2003) Two decades of global tsunamis: 1982–2002. Sci Tsunami Hazards 21:3–88

Lastras G, Amblas D, Calafat AM, Canals M, Frigola J, Hermanns RL, Lafuerza S, Longva O, Micallef A, Sepúlveda SA, Vargas G, Batist MD, van Daele M, Azpiroz M, Bascuñán I, Duhart P, Iglesias O, Kempf P, Rayo X (2013) Landslides cause tsunami waves: insights from aysén fjord, Chile. Eos Trans AGU 94:297–298. https://doi.org/10.1002/2013EO340002

Latter JH (1981) Tsunamis of volcanic origin: summary of causes, with particular reference to krakatoa, 1883. Bull Volcanol 44:467–490. https://doi.org/10.1007/BF02600578

Lausitzer und Mitteldeutsche Bergbau-Verwaltungsgesellschaft (ed) (2020) The rehabilitation of the Nachterstedt opencast mine after the embankment movement of 2009. (in German language), Leipzig

Li S, Xu Q, Tang M, Iqbal J, Liu J, Zhu X, Liu F, Zhu D (2019) Characterizing the Spatial distribution and fundamental controls of landslides in the three Gorges reservoir area, China. Bull Eng Geol Environ 78:4275–4290. https://doi.org/10.1007/s10064-018-1404-5

Lin CH, Kumagai H, Ando M, Shin TC (2010) Detection of landslides and submarine slumps using broadband seismic networks. Geophys Res Lett 37. https://doi.org/10.1029/2010GL044685

Liu PL-F, Higuera P, Husrin S, Prasetya GS, Prihantono J, Diastomo H, Pryambodo DG, Susmoro H (2020) Coastal landslides in palu Bay during 2018 Sulawesi earthquake and tsunami. Landslides 17:2085–2098. https://doi.org/10.1007/s10346-020-01417-3

Liu Z, L'Heureux J-S, Glimsdal S, Lacasse S (2021) Modelling of mobility of Rissa landslide and following tsunami. Comput Geotech 140:104388. https://doi.org/10.1016/j.compgeo.2021.104388

Løvholt F, Pedersen G, Harbitz CB, Glimsdal S, Kim J (2015) On the characteristics of landslide tsunamis. Philos Trans Math Phys Eng Sci 373. https://doi.org/10.1098/rsta.2014.0376

Løvholt F, Glimsdal S, Harbitz CB (2020) On the landslide tsunami uncertainty and hazard. Landslides 17:2301–2315. https://doi.org/10.1007/s10346-020-01429-z

Lüthi MP, Vieli A (2016) Multi-method observation and analysis of a tsunami caused by glacier calving. Cryosphere 10:995–1002. https://doi.org/10.5194/tc-10-995-2016

Maciel GF, Pereira JB, Sáo YT, Ferreira FO, Ferreira LG (2023) Impulse wave in the Brazilian Lake of Capitólio. RBRH 28. https://doi.org/10.1590/2318-0331.282320230036

Maramai A, Brizuela B, Graziani L (2014) The Euro-Mediterranean tsunami catalogue. Ann Geophys 57. https://doi.org/10.4401/ag-6437

Marchenko AV, Morozov EG, Muzylev SV (2012) A tsunami wave recorded near a glacier front. Nat Hazards Earth Syst Sci 12:415–419. https://doi.org/10.5194/nhess-12-415-2012
Matsuoka N, Murton J (2008) Frost weathering: recent advances and future directions. Permafr Periglac Process 19:195–210. https://doi.org/10.1002/ppp.620
McColl ST (2012) Paraglacial rock-slope stability. Geomorphology 153–154:1–16. https://doi.org/10.1016/j.geomorph.2012.02.015
McColl ST, Cook SJ (2024) A universal size classification system for landslides. Landslides 21:111–120. https://doi.org/10.1007/s10346-023-02131-6
Miller DJ (1960) Giant waves in Lituya Bay, Alaska: Geological Survey Professional Paper 354-C, Washington
Mitchell RC (1954) Submarine landslips off the Coasts of Puerto Rico and barbados, West Indies. Nature 173:119–121. https://doi.org/10.1038/173119a0
Miyamoto K (2010) Numerical simulation of landslide movement and Unzen-Mayuyama disaster in 1792, Japan. J Disaster Res 5:280–287. https://doi.org/10.20965/jdr.2010.p0280
Muhari A, Imamura F, Arikawa T, Hakim AR, Afriyanto B (2018) Solving the puzzle of the September 2018 palu, indonesia, tsunami mystery: clues from the tsunami waveform and the initial field survey data. J Disaster Res 13. https://doi.org/10.20965/jdr.2018.sc20181108
Murty TS (2003) Tsunami wave height dependence on landslide volume. Pure Appl Geophys 160:2147–2153. https://doi.org/10.1007/s00024-003-2423-z
Naranjo JA, Arenas M, Clavero J, Muñoz O (2009) Mass movement-induced tsunamis: main effects during the Patagonian Fjordland seismic crisis in Aisén (45°25'S), Chile. Andean Geol 36:137–145
National Geophysical Data Center (2024) NCEI/WDS global historical tsunami database. https://doi.org/10.7289/V5PN93H7
Neumann P (2023) Cause of rockfall at Waldenecksee near Baden-Baden clarified: geologist has examined quarry. (in German language). SWR Aktuell Baden-Württemberg. https://www.swr.de/swraktuell/baden-wuerttemberg/karlsruhe/ursache-felssturz-waldenecksee-bei-baden-baden-100.html
Nigg V, Wohlwend S, Hilbe M, Bellwald B, Fabbri SC, de Souza GF, Donau F, Grischott R, Strasser M, Anselmetti FS (2021) A tsunamigenic delta collapse and its associated tsunami deposits in and around lake sils, Switzerland. Nat Hazards 9:1897. https://doi.org/10.1007/s11069-021-04533-y
Nomanbhoy N, Satake K (1995) Generation mechanism of tsunamis from the 1883 Krakatau eruption. Geophys Res Lett 22:509–512. https://doi.org/10.1029/94GL03219
Normandeau A, MacKillop K, Macquarrie M, Richards C, Bourgault D, Campbell DC, Maselli V, Philibert G, Clarke JH (2021) Submarine landslides triggered by iceberg collision with the seafloor. Nat Geosci 14:599–605. https://doi.org/10.1038/s41561-021-00767-4
Okal EA, Synolakis CE (2003) A theoretical comparison of tsunamis from dislocations and landslides. Pure Appl Geophys 160:2177–2188. https://doi.org/10.1007/s00024-003-2425-x
Okal EA, Fryer GJ, Borrero JC, Ruscher C (2002) The landslide and local tsunami of 13 September 1999 on Fatu Hiva (Marquesas islands; French Polynesia). Bull Soc Géol France 173:359–367. https://doi.org/10.2113/173.4.359
Omira R, Dogan GG, Hidayat R, Husrin S, Prasetya GS, Annunziato A, Proietti C, Probst P, Paparo MA, Wronna M, Zaytsev AI, Pronin PI, Giniyatullin A, Putra PS, Hartanto D, Ginanjar G, Kongko W, Pelinovsky EN, Yalçiner AC (2019) The September 28th, 2018, tsunami in Palu-Sulawesi, indonesia: A Post-Event field survey. Pure Appl Geophys 176:1379–1395. https://doi.org/10.1007/s00024-019-02145-z
Panthi KK, Nilsen B (2006) Numerical analysis of stresses and displacements for the Tafjord slide. Nor Bull Eng Geol Environ 65:57–63. https://doi.org/10.1007/s10064-005-0009-y
Papadopoulos GA, Chalkis BJ (1984) Tsunamis observed in Greece and the surrounding area from antiquity up to the present times. Mar Geol 56:309–317. https://doi.org/10.1016/0025-3227(84)90022-7
Papadopoulos GA, Daskalaki E, Fokaefs A (2007) Tsunamis generated by coastal and submarine landslides in the Mediterranean Sea. https://doi.org/10.1007/978-1-4020-6512-5_43. In: Lykousis V, Sakellariou D, Locat J (eds) Submarine mass movements and their consequences. Springer Netherlands, Dordrecht, pp 415–422
Paris R, Switzer AD, Belousova M, Belousov A, Ontowirjo B, Whelley PL, Ulvrova M (2014) Volcanic tsunami: A review of source mechanisms, past events and hazards in Southeast Asia (Indonesia, philippines, Papua new Guinea). Nat Hazards 70:447–470. https://doi.org/10.1007/s11069-013-0822-8
Paris A, Okal EA, Guérin C, Heinrich P, Schindelé F, Hébert H (2019) Numerical modeling of the June 17, 2017 landslide and tsunami events in Karrat fjord, West Greenland. Pure Appl Geophys 176:3035–3057. https://doi.org/10.1007/s00024-019-02123-5
Pedrosa-González MT, González-Vida JM, Galindo-Záldivar J, Ortega S, Castro MJ, Casas D, Ercilla G (2022) Simulation of tsunami induced by a submarine landslide in a glaciomarine margin: the case of Storfjorden LS-1 (southwestern Svalbard Islands). Nat Hazards Earth Syst Sci 22:3839–3858. https://doi.org/10.5194/nhess-22-3839-2022

Pelinovsky EN, Mazova RK (1992) Exact analytical solutions of nonlinear problems of tsunami wave run-up on slopes with different profiles. Nat Hazards 6:227–249. https://doi.org/10.1007/BF00129510
Petley DN (2009) 38 years ago today – the Chungar landslide in Peru. https://blogs.agu.org/landslideblog/2009/03/18/38-years-ago-today-the-chungar-landslide-in-peru/. Accessed 11 December 2024
Petley DN (2020) Bute Inlet: a very long runout proglacial landslide in Canada. https://blogs.agu.org/landslideblog/2020/12/16/bute-inlet-landslide/. Accessed 16 December 2024
Petley DN (2022) The 1979 Nice Airport landslide and tsunami. https://blogs.agu.org/landslideblog/2022/02/04/nice-airport-1/. Accessed 11 December 2024
Plafker G, Eyzaguirre VR (1979) Rock avalanche and wave at Chungar, Peru. https://doi.org/10.1016/B978-0-444-41508-0.50015-6. In: Voight B (ed) Rockslides and avalanches, 2: Engineering sites, vol 14. Elsevier, pp 269–279
Pranantyo IR, Cummins PR (2020) The 1674 Ambon tsunami: extreme run-up caused by an earthquake-triggered landslide. Pure Appl Geophys 177:1639–1657. https://doi.org/10.1007/s00024-019-02390-2
Prior DB, Bornhold BD, Coleman JM, Bryant WR (1982) Morphology of a submarine slide, Kitimat arm, British Columbia. Geol 10:588. https://doi.org/10.1130/0091-7613(1982)10<588:MOASSK>2.0.CO;2
Rabinovich AB, Thomson RE, Kulikov EA, Bornhold BD, Fine IV (1999) The landslide-generated tsunami of November 3, 1994 in Skagway harbor, alaska: A case study. Geophys Res Lett 26:3009–3012. https://doi.org/10.1029/1999GL002334
Ranguelov B, Tinti S, Pagnoni G, Tonini R, Zaniboni F, Armigliato A (2008) The nonseismic tsunami observed in the Bulgarian black sea on 7 May 2007: was it due to a submarine landslide? Geophys Res Lett 35. https://doi.org/10.1029/2008GL034905
Reichenbach P, Rossi M, Malamud BD, Mihir M, Guzzetti F (2018) A review of statistically-based landslide susceptibility models. Earth-Sci Rev 180:60–91. https://doi.org/10.1016/j.earscirev.2018.03.001
Roberts NJ, McKillop RJ, Hermanns RL, Clague JJ, Oppikofer T (2014) Preliminary global catalogue of displacement waves from subaerial landslides. In: Sassa K, Canuti P, Yin Y (eds) Landslide science for a safer geo-environment: volume 3: targeted landslides. Springer, Cham
Roger JH, Bull S, Watson SJ, Mueller C, Hillman JI, Wolter A, Lamarche G, Power W, Lane E, Woelz S, Davidson S (2024) A review of approaches for submarine landslide-tsunami hazard identification and assessment. Mar Pet Geol 162:106729. https://doi.org/10.1016/j.marpetgeo.2024.106729
Rosenqvist IT (1953) Considerations on the sensitivity of Norwegian quick-clays. Géotechnique 3:195–200. https://doi.org/10.1680/geot.1953.3.5.195
Rudolphi M (2023) Rockfall at Waldenecksee near Baden-Baden leaves trail of devastation: Area is closed. (in German language). Badische Neueste Nachrichten. https://bnn.de/mittelbaden/baden-baden/felssturz-am-waldenecksee-bei-baden-baden-loest-spur-der-verwuestung-aus
Rynn J (2002) A preliminary assessment of tsunami hazard and risk in the Indonesian region. Sci Tsunami Hazards 20:193–215
Sassa K, Canuti P, Yin Y (eds) (2014) Landslide science for a safer geo-environment: volume 3: targeted landslides. Springer, Cham
Schiermeier Q (2017) Huge landslide triggered rare Greenland mega-tsunami. Nature. https://doi.org/10.1038/nature.2017.22374
Schindelé F, Kong L, Lane EM, Paris R, Ripepe M, Titov V, Bailey R (2024) A review of tsunamis generated by volcanoes (TGV) source mechanism, modelling, monitoring and warning systems. Pure Appl Geophys 181:1745–1792. https://doi.org/10.1007/s00024-024-03515-y
Schubert C (1994) Tsunamis in Venezuela: some observations on their occurrence. Journal of Coastal Research Special Issue No. 12. Coastal Hazards: Perception, Susceptibility, and Mitigation:189–195
Schulten I, Mosher DC, Piper DJW, Krastel S (2019) A massive slump on the st. Pierre slope, a new perspective on the 1929 grand banks submarine landslide. J Geophys Res Solid Earth 124:7538–7561. https://doi.org/10.1029/2018JB017066
Sedore P, Normandeau A, Maselli V (2024) Environmental controls on the generation of submarine landslides in Arctic fjords: insight from Pangnirtung fjord, Baffin Island. Nunavut Mar Geol 472:107290. https://doi.org/10.1016/j.margeo.2024.107290
Seed HB, Seed RB, Schlosser F, Blondeau F, Juran I (1988) The landslide at the Port of Nice on October 16, 1979, Earthquake Engineering Research Center (University of California, Berkeley), Report No. UCB/EERC-88/10. https://nehrpsearch.nist.gov/static/files/NSF/PB91210914.pdf. Accessed 9 August 2023
Sepúlveda SA, Serey A (2009) Tsunamigenic, earthquake-triggered rock slope failures during the April 21, 2007 Aisén earthquake, Southern Chile (45.5°S). Andean Geol 36:131–136. https://doi.org/10.5027/andgeoV36n1-a10
Sepúlveda SA, Serey A, Lara M, Pavez A, Rebolledo S (2010) Landslides induced by the April 2007 aysén Fjord earthquake, Chilean patagonia. Landslides 7:483–492. https://doi.org/10.1007/s10346-010-0203-2

Shrestha F, Steiner JF, Shrestha R, Dhungel Y, Joshi SP, Inglis S, Ashraf A, Wali S, Walizada KM, Zhang T (2023) A comprehensive and version-controlled database of glacial lake outburst floods in high mountain Asia. Earth Syst Sci Data 15:3941–3961. https://doi.org/10.5194/essd-15-3941-2023

Soloviev SL, Go CN (1974) Catalogue of tsunamis on the Western shore of the Pacific ocean. Nauka Publishing House, Moscow

Soloviev SL, Go CN (1975) Catalogue of tsunamis on the eastern shore of the Pacific Ocean (1513–1968). Can. Transi. Fish. Aquat. Sci. 5078. Nauka Publishing House, Moscow, USSR

Soloviev SL, Solovieva ON, Go CN, Kim KS, Shchetnikov NA, Bonnin J, Levin BW, Tinti S, Papadopoulos GA (2000) Tsunamis in the mediterranean sea 2000 B.C.–2000 A.D, vol 13. Springer Netherlands, Dordrecht

Sosio R, Crosta GB, Hungr O (2012) Numerical modeling of debris avalanche propagation from collapse of volcanic edifices. Landslides 9:315–334. https://doi.org/10.1007/s10346-011-0302-8

Spahn H, Lauterjung J (2023) Tsunami preparedness in Indonesia with special consideration of landslide and volcanic induced events: characterization of the Threat - What do communities in risk areas need to be prepared for? Sci Tech Rep STR23/07. https://doi.org/10.48440/GFZ.B103-23079

Straume EO, Gaina C, Medvedev S, Hochmuth K, Gohl K, Whittaker JM, Abdul Fattah R, Doornenbal JC, Hopper JR (2019) GlobSed: updated total sediment thickness in the world's oceans. Geochem Geophys Geosyst 20:1756–1772. https://doi.org/10.1029/2018GC008115

Svennevig K, Hicks SP, Forbriger T, Lecocq T, Widmer-Schnidrig R, Mangeney A, Hibert C, Korsgaard NJ, Lucas A, Satriano C, Anthony RE, Mordret A, Schippkus S, Rysgaard S, Boone W, Gibbons SJ, Cook KL, Glimsdal S, Løvholt F, van Noten K, Assink JD, Marboeuf A, Lomax A, Vanneste K, Taira T, Spagnolo M, de Plaen R, Koelemeijer P, Ebeling C, Cannata A, Harcourt WD, Cornwell DG, Caudron C, Poli P, Bernard P, Larose E, Stutzmann E, Voss PH, Lund B, Cannavo F, Castro-Díaz MJ, Chaves E, Dahl-Jensen T, de Pinho Dias N, Déprez A, Develter R, Dreger D, Evers LG, Fernández-Nieto ED, Ferreira AMG, Funning G, Gabriel A-A, Hendrickx M, Kafka AL, Keiding M, Kerby J, Khan SA, Dideriksen AK, Lamb OD, Larsen TB, Lipovsky B, Magdalena I, Malet J-P, Myrup M, Rivera L, Ruiz-Castillo E, Wetter S, Wirtz B (2024) A rockslide-generated tsunami in a Greenland Fjord Rang Earth for 9 days. Science 385:1196–1205. https://doi.org/10.1126/science.adm9247

Synolakis CE, Bardet J-P, Borrero JC, Davies HL, Okal EA, Silver EA, Sweet S, Tappin DR (2002) The slump origin of the 1998 Papua new Guinea tsunami. Proc R Soc Lond A 458:763–789. https://doi.org/10.1098/rspa.2001.0915

Taira A (2001) Tectonic evolution of the Japanese Island Arc system. Annu Rev Earth Planet Sci 29:109–134. https://doi.org/10.1146/annurev.earth.29.1.109

Tang H, Li C, Hu X, Su A, Wang L, Wu Y, Criss R, Xiong C, Li Y (2015) Evolution characteristics of the Huangtupo landslide based on in situ tunneling and monitoring. Landslides 12:511–521. https://doi.org/10.1007/s10346-014-0500-2

Tang H, Wasowski J, Juang CH (2019) Geohazards in the three Gorges reservoir area, China – Lessons learned from decades of research. Eng Geol 261:105267. https://doi.org/10.1016/j.enggeo.2019.105267

ten Brink US, Geist EL (2021) On the use of statistical analysis to understand submarine landslide processes and assess their hazard. https://doi.org/10.1007/978-3-030-60196-6_23. In: Sassa K, Mikoš M, Sassa S, Bobrowsky PT, Takara K, Dang K (eds) Understanding and reducing landslide disaster risk: Volume 1 - Sendai Landslide partnerships and Kyoto Landslide Commitment. Springer International Publishing, Cham, pp 329–341

Tinti S, Manucci A, Pagnoni G, Armigliato A, Zaniboni F (2005) The 30 December 2002 landslide-induced tsunamis in stromboli: sequence of the events reconstructed from the eyewitness accounts. Nat Hazards Earth Syst Sci 5:763–775. https://doi.org/10.5194/nhess-5-763-2005

TL/ICMMG (2024) Global Historical Tsunami Database. Tsunami Laboratory, Institute of Computational Mathematics and Mathematical Geophysics of Siberian Division of Russian Academy of Sciences, Novosibirsk, Russia. http://tsun.sscc.ru/gtdb/default.aspx. Accessed 28 October 2024

Urgeles R, Camerlenghi A (2013) Submarine landslides of the mediterranean sea: trigger mechanisms, dynamics, and frequency-magnitude distribution. J Geophys Res Earth Surf 118:2600–2618. https://doi.org/10.1002/2013JF002720

USGS (2024) 2024 Pedersen Lagoon landslide-generated tsunami. https://www.usgs.gov/programs/landslide-hazards/science/2024-pedersen-lagoon-landslide-generated-tsunami#overview. Accessed 6 September 2024

van Daele M, Versteeg W, Pino M, Urrutia R, Batist MD (2013) Widespread deformation of basin-plain sediments in aysén Fjord (Chile) due to impact by earthquake-triggered, onshore-generated mass movements. Mar Geol 337:67–79. https://doi.org/10.1016/j.margeo.2013.01.006

van den Gardner JV, Gelfenbaum G, Barnhardt W, Lee HJ, Palmer S (2001) Mapping southern Puget Sound Delta fronts after the 2001 Nisqually earthquake. U.S. Geological Survey Open File Report. https://pubs.usgs.gov/of/2001/0266/. Accessed 19 August 2024

Vera F, Tilmann F, Saul J, Karyono, Babeyko A (2025) Seismic-based detection, location and identification of volcano-induced landslides: a feasibility study based on the 2018 Anak Krakatau volcano flank collapse. Nat Hazards. https://doi.org/10.1007/s11069-025-07465-z

Vilibić I, Šepić J, Ranguelov B, Mahović NS, Tinti S (2010) Possible atmospheric origin of the 7 May 2007 Western black sea shelf tsunami event. J Geophys Res 115. https://doi.org/10.1029/2009JC005904

Völker D, Scholz F, Geersen J (2011) Analysis of submarine landsliding in the rupture area of the 27 February 2010 Maule earthquake, central Chile. Mar Geol 288:79–89. https://doi.org/10.1016/j.margeo.2011.08.003

von Huene R, Bourgois J, Miller J, Pautot G (1989) A large Tsunamogenic landslide and debris flow along the Peru trench. J Geophys Res 94:1703–1714. https://doi.org/10.1029/JB094iB02p01703

Walden J, Jacquemart M, Higman B, Hugonnet R, Manconi A, Farinotti D (2025) Landslide activation during deglaciation in a Fjord dominated landscape: observations from Southern Alaska (1984–2022). Nat Hazards Earth Syst Sci 25:2045–2073. https://doi.org/10.5194/nhess-25-2045-2025

Walter TR, Haghshenas Haghighi M, Schneider FM, Coppola D, Motagh M, Saul J, Babeyko AY, Dahm T, Troll VR, Tilmann F, Heimann S, Valade S, Triyono R, Khomarudin R, Kartadinata N, Laiolo M, Massimetti F, Gaebler P (2019) Complex hazard cascade culminating in the Anak Krakatau sector collapse. Nat Commun 10:4339. https://doi.org/10.1038/s41467-019-12284-5

Waltham T (2002) Unloading joints and rockfalls in norway's fiordlands. Geol Today 18:220–225. https://doi.org/10.1046/j.0266-6979.2003.00374.x

Wang J, Schweizer D, Liu Q, Su A, Hu X, Blum P (2021a) Three-dimensional landslide evolution model at the Yangtze river. Eng Geol 292:106275. https://doi.org/10.1016/j.enggeo.2021.106275

Wang J, Wang S, Su A, Xiang W, Xiong C, Blum P (2021b) Simulating landslide-induced tsunamis in the Yangtze river at the three Gorges in China. Acta Geotech 16:2487–2503. https://doi.org/10.1007/s11440-020-01131-3

Wang J, Xiao L, Ward SN, Du J (2021c) Tsunami squares modeling of the 2007 dayantang landslide generated waves considering the effects in slide/water interactions. Eng Geol 284:106032. https://doi.org/10.1016/j.enggeo.2021.106032

Wang X, Yin Y, Zhang Z, Huang B, Wang L, Zhao P, Yi Z (2024) Potential failure mechanism and tsunami risk analysis of the longmen dangerous rock mass in the scenic area within the three Gorges reservoir area, China. Nat Hazards 120:9421–9444. https://doi.org/10.1007/s11069-024-06560-x

Wieczorek GF (1996) Landslide triggering mechanisms. In: Turner AK, Schuster RL (eds) Landslides: investigation and mitigation. National Academy, Washington D.C.

Xing A, Xu Q, Zhu Y, Zhu J, Jiang Y (2016) The August 27, 2014, rock avalanche and related impulse water waves in Fuquan. Guizhou China Landslides 13:411–422. https://doi.org/10.1007/s10346-016-0679-5

Yamada Y, Kawamura K, Ikehara K, Ogawa Y, Urgeles R, Mosher D, Chaytor JD, Strasser M (eds) (2012) Submarine mass movements and their consequences: 5th International Symposium. Advances in natural and technological hazards research, vol 31. Springer Science+Business Media B.V, Dordrecht

Yang W, Yang T, Ying C, De-ying L, Wei W (2014) Study on the velocity of partially submerged landslide. JESTR 7:62–67. https://doi.org/10.25103/jestr.073.10

Yang B, Yin K, Xiao T, Chen L, Du J (2017) Annual variation of landslide stability under the effect of water level fluctuation and rainfall in the three Gorges reservoir, China. Environ Earth Sci 76. https://doi.org/10.1007/s12665-017-6898-9

Yin Y, Wang H, Gao Y, Li X (2010) Real-time monitoring and early warning of landslides at relocated Wushan town, the three Gorges reservoir, China. Landslides 7:339–349. https://doi.org/10.1007/s10346-010-0220-1

Zaniboni F, Armigliato A, Pagnoni G, Tinti S (2014) Continental margins as a source of tsunami hazard: the 1977 Gioia Tauro (Italy) landslide–tsunami investigated through numerical modeling. Mar Geol 357:210–217. https://doi.org/10.1016/j.margeo.2014.08.011

Zhang Z, He S, Liu W, Liang H, Yan S, Deng Y, Bai X, Chen Z (2019) Source characteristics and dynamics of the October 2018 Baige landslide revealed by broadband seismograms. Landslides 16:777–785. https://doi.org/10.1007/s10346-019-01145-3

Zhou J, Xu F, Yang X, Yang Y, Lu P (2016) Comprehensive analyses of the initiation and landslide-generated wave processes of the 24 June 2015 Hongyanzi landslide at the three Gorges reservoir, China. Landslides 13:589–601. https://doi.org/10.1007/s10346-016-0704-8